mitochondrial enzymes from *Plasmodium* (Krungkrai, 1995, 1997). However, we have found that the purity of the mitochondrial sample prepared by the nitrogen cavitation method could not be improved by the method Fry and Beesley reported (1991). Instead, longer centrifugation with stronger force resulted in a better separation of the mitochondrion (23% (v/v) Percoll, 100,000*g* for 1 h). It is probably because each subcellular structure in the cell was less damaged by nitrogen cavitation in our method than the homogenization with glass-Teflon homogenizer by Fry and Beesley (1991). Indeed, the intact food vacuole containing haemozoin crystals was observed even after our fractionation method (Fig. 3F), and we previously noted that the mitochondrial activity represented by the succinate dehydrogenase was 2 to 3 times higher in of the crude mitochondrial preparation prepared by nitrogen cavitation (Takashima et al., 2001) than those prepared by other conventional methods (Suraveratum et al., 2000).

In this study, the DHOD-specific activity increased about 5 times after the Percoll density gradient centrifugation in the second peak (Fig. 2B), indicating that the contaminants were removed. Indeed, the observation by the electron microscope showed that hemozoin and food vacuole were significantly reduced after the Percoll density gradient centrifugation. Electron microscopic analysis confirmed that the mitochondrion with double membrane was enriched in the fractions forming the second peak (Fig. 3C and D).

Unlike the food vacuole, the apicoplast was not separated from the mitochondrion after the Percoll density gradient centrifugation. It might be because the organelle, by chance, shares the similar density with the mitochondrion. We examined this possibility by a different fractionation method – fluorescence-activated organelle sorting (FOS). Single organelle sorting has been applied to various organelles to determine the characteristics of individual organelle (Böck et al., 1997). The use of fluorescent organelle cytometry attracted scientists' attention to study single mitochondria (Cavelier et al., 2000). In this study, we took the advantage of single organelle sorting to improve the purity of mitochondria sample. After the FOS, the presence of the mitochondrion and the apicoplast genomic DNAs in the GFP positive fraction recovered was confirmed by PCR with target specific primers. This result indicates that applying different mode of fractionation, mitochondria and apicoplast were, again, co-fractionated. Our results strongly suggest that the mitochondrion and the apicoplast of *P. falciparum* are bound to each other.

Up to date, study of mitochondrion and apicoplast of *Plasmodium* has been restricted to the whole cell, and physical interaction between two organelles had not been determined. The extensive genomic information from malaria genome project (Gardner et al., 2002) provided ideas about the putative metabolic pathway in mitochondria and apicoplast in *P. falciparum*. Among those pathways, heme biosynthesis is unique one as the pathway is predicted to begin in the mitochondrion but subsequent reactions are likely taken place in the apicoplast; 5-aminolevulinic acid (ALA), the first intermediate of the pathway, seemed to be synthesized in the mitochondrion via Shemin pathway but converted to porphobilinogen, the next intermediate, in the apicoplast. This peculiarity was experimentally confirmed by localizing ALA synthase and porphobilinogen synthase (ALA dehydratase), respectively (Sato et al., 2004). The parasite may have a requirement to locate these two organelles in a close proximity to facilitate transport of ALA from the mitochondrion to the apicoplast.

The mitochondrion and the apicoplast of *Plasmodium* spp. have been observed in a proximity to each other by electron microscopy and fluorescent microscopy (Aikawa, 1966; Hopkins et al., 1999; Sato et al., 2004; van Dooren et al., 2005), however the strength in the interaction might vary depending on the parasite stage. It is possible that interaction between apicoplast and mitochondrion to be disrupted in the process of mitochondria preparation.

Despite of extensive observations, it is still unknown if there is a significant structure directly connecting these organelles, like tight junction. These organelles can be connected indirectly, e.g., through the cytoskeleton. Both organelles were recovered not only in the fractions forming the second peak with the DHOD activity but also in those forming the first peak after our Percoll centrifugation (Fig. 2). This may suggest that the putative connection between the organelles has a complex structure involving plenty of auxiliary proteins in a physiological state, but can be reduced to a simple, basic structure that is still capable to hold both organelles together.

Acknowledgements

The authors thank late Dr. Masamichi Aikawa for comments on morphological observations by electron microscopy and wish to dedicate this paper to him. The blood and plasma used in this study is a kind donation from Tokyo Metropolitan Red Cross Blood Centre. WR99210, the drug used for the screening of transfected parasites was a kind gift from Jacobus Pharmaceutical Co., Inc. This study was supported by a Grant-in-Aid for scientific research on priority areas and for Creative Scientific Research from the Japanese Ministry of Education, Science, Culture, and Sports (13226015, 13854011, 17209013, 17590368, 18073004 and 18GS0314) and for research on emerging and re-emerging infectious diseases from the Japanese Ministry of Health and Welfare, and by British Medical Research Council.

References

Aikawa, M., 1966. The fine structure of the erythrocytic stages of three avian malarial parasites, *Plasmodium fallax*, *P. lophurae* and *P. cathemerium*. Am. J. Trop. Med. Hyg. 15, 449–471.

Bannister, L.H., Hopkins, J.M., Fowler, R.E., Krishna, S., Mitchell, G.H., 2000. A brief illustrated guide to the ultrastructure of *Plasmodium falciparum* asexual blood stages. Parasitol. Today 16, 427–433.

Böck, G., Steinlein, P., Huber, L.A., 1997. Cell biologists sort things out: analysis and purification of intracellular organelles by flow cytometry. Trends Cell Biol. 7, 499–503.

Bradford, M.M., 1976. A rapid and sensitive method for the quantitation of microgram quantities of protein utilizing the principle of protein–dye binding. Anal. Biochem. 72, 248–254.

Cavelier, L., Johannisson, A., Gyllensten, U., 2000. Analysis of mtDNA copy number and composition of single mitochondrial particles using flow cytometry and PCR. Exp. Cell Res. 259, 79–85.

Feagin, J.E., 1992. The 6-kb element of *Plasmodium falciparum* encodes mitochondrial cytochrome genes. Mol. Biochem. Parasitol. 52, 145–148.

Fry, M., Beesley, J.E., 1991. Mitochondria of mammalian *Plasmodium* spp.. Parasitology 102, 17–26.

Gardner, M.J., Hall, N., Fung, E., White, O., Berriman, M., Hyman, R.W., Carlton, J.M., Pain, A., Nelson, K.E., Bowman, S., Paulsen, I.T., James, K., Eisen, J.A., Rutherford, K., Salzberg, S.L., Craig, A., Kyes, S., Chan, M.S., Nene, V., Shallom, S.J., Suh, B., Peterson, J., Angiuoli, S., Pertea, M., Allen, J., Selengut, J., Haft, D., Mather, M.W., Vaidya, A.B., Martin, D.M., Fairlamb, A.H., Fraunholz, M.J., Roos, D.S., Ralph, S.A., McFadden, G.I., Cummings, L.M., Subramanian, G.M., Mungall, C., Venter, J.C., Carucci, D.J., Hoffman, S.L., Newbold, C., Davis, R.W., Fraser, C.M., Barrell, B., 2002. Genome sequence of the human malaria parasite *Plasmodium falciparum*. Nature 419, 498–511.

Gardner, M.J., Bishop, R., Shah, T., de Villiers, E.P., Carlton, J.M., Hall, N., Ren, Q., Paulsen, I.T., Pain, A., Berriman, M., Wilson, R.J.M., Sato, S., Ralph, S.A., Mann, D.J., Xiong, Z., Shallom, S.J., Weidman, J., Jiang, L., Lynn, J., Weaver, B., Shoaibi, A., Domingo, A.R., Wasawo, D., Crabtree, J., Wortman, J.R., Haas, B., Angiuoli, S.V., Creasy, T.H., Lu, C., Suh, B., Silva, J.C., Utterback, T.R., Feldblyum, T.V., Pertea, M., Allen, J., Nierman, W.C., Taracha, E.L., Salzberg, S.L., White, O.R., Fitzhugh, H.A., Morzaria, S., Venter, J.C., Fraser, C.M., Nene, V., 2005. Genome sequence of *Theileria parva*, a bovine pathogen that transforms lymphocytes. Science 309, 134–137.

Gero, A.M., Brown, G.V., O'Sullivan, W.J., 1984. Pyrimidine de novo synthesis during the life cycle of the intraerythrocytic stage of *Plasmodium falciparum*. J. Parasitol. 70, 536–541.

Greenwood, B.M., Bojang, K., Whitty, C.J., Targett, G.A., 2005. Malaria. Lancet 365, 487–498.

Gutteridge, W.E., Trigg, P.I., 1970. Incorporation of radioactive precursors into DNA and RNA of *Plasmodium knowlesi in vitro*. J. Protozool. 17, 89–96.

Hopkins, J., Fowler, R., Krishna, S., Wilson, I., Mitchell, G., Bannister, L., 1999. The plastid in *Plasmodium falciparum* asexual blood stages: a three-dimensional ultrastructural analysis. Protist 150, 283–295.

Kohler, S., Delwiche, C.F., Denny, P.W., Tilney, L.G., Webster, P., Wilson, R.J.M., Palmer, J.D., Roos, D.S., 1997. A plastid of probable green algal origin in Apicomplexan parasites. Science 275, 1485–1489.

Krungkrai, J., 1995. Purification, characterization and localization of mitochondrial dihydroorotate dehydrogenase in *Plasmodium falciparum*, human malaria parasite. Biochim. Biophys. Acta 1243, 351–360.

Krungkrai, J., Krungkrai, S.R., Suraveratum, N., Prapunwattana, P., 1997. Mitochondrial ubiquinol-cytochrome *c* reductase and cytochrome *c* oxidase: chemotherapeutic targets in malarial parasites. Biochem. Mol. Biol. Int. 42, 1007–1014.

Lambros, C., Vanderberg, J.P., 1979. Synchronization of *Plasmodium falciparum* erythrocytic stages in culture. J. Parasitol. 65, 418–420.

Mi-Ichi, F., Miyadera, H., Kobayashi, T., Takamiya, S., Waki, S., Iwata, S., Shibata, S., Kita, K., 2005. Parasite mitochondria as a target of chemotherapy: inhibitory effect of licochalcone A on the *Plasmodium falciparum* respiratory chain. Ann. N. Y. Acad. Sci. 1056, 46–54.

Prapunwattana, P., O'sullivan, W.J., Yuthavong, Y., 1988. Depression of *Plasmodium falciparum* dihydroorotate dehydrogenase activity in *in vitro* culture by tetracycline. Mol. Biochem. Parasitol. 27, 119–124.

Ralph, S.A., van Dooren, G.G., Waller, R.F., Crawford, M.J., Fraunholz, M.J., Foth, B.J., Tonkin, C.J., Roos, D.S., McFadden, G.I., 2004. Metabolic maps and functions of the *Plasmodium falciparum* apicoplast. Nat. Rev. 2, 203–216.

Roth Jr., E.F., Calvin, M.C., Max-Audit, I., Rosa, J., Rosa, R., 1988. The enzymes of the glycolytic pathway in erythrocytes infected with *Plasmodium falciparum* malaria parasites. Blood 72, 1922–1925.

Sato, S., Rangachari, K., Wilson, R.J.M., 2003. Targeting GFP to the malarial mitochondrion. Mol. Biochem. Parasitol. 130, 155–158.

Sato, S., Clough, B., Coates, L., Wilson, R.J., 2004. Enzymes for heme biosynthesis are found in both the mitochondrion and plastid of the malaria parasite *Plasmodium falciparum*. Protist 155, 117–125.

Sherman, I.W., 1979. Biochemistry of Plasmodium (malaria parasite). Microbiol. Rev. 43, 453–495.

Srivastava, I.K., Rottenberg, H., Vaidya, A.B., 1997. Atovaquone, a broad spectrum antiparasitic drug, collapses mitochondrial membrane potential in a malarial parasite. J. Biol. Chem. 272, 3961–3966.

Srivastava, I.K., Morrisey, J.M., Darrouzet, E., Daldal, F., Vaidya, A.B., 1999. Resistance mutations reveal the atovaquone-binding domain of cytochrome *b* in malaria parasites. Mol. Microbiol. 33, 704–711.

Slomianny, C., Prensier, G., 1986. Application of the serial sectioning and tridimensional reconstruction techniques to the morphological study of the *Plasmodium falciparum* mitochondrion. J. Parasitol. 72, 595–598.

Suraveratum, N., Krungkrai, S.R., Leangaramgul, P., Prapunwattana, P., Krungkrai, J., 2000. Purification and characterization of *Plasmodium falciparum* succinate dehydrogenase. Mol. Biochem. Parasitol. 105, 215–222.

Takashima, E., Takamiya, S., Takeo, S., Mi-ichi, F., Amino, H., Kita, K., 2001. Isolation of mitochondria from *Plasmodium falciparum* showing dihydroorotate dependent respiration. Parasitol. Int. 50, 273–278.

Takeo, S., Kokaze, A., Ng, C.S., Mizuchi, D., Watanabe, J.I., Tanabe, K., Kojima, S., Kita, K., 2000. Succinate dehydrogenase in *Plasmodium falciparum* mitochondria: molecular characterization of the SDHA and SDHB genes for the catalytic subunits, the flavoprotein (Fp) and iron–sulfur (Ip) subunits. Mol. Biochem. Parasitol. 107, 191–205.

Tan, T.M., Nelson, J.S., Ng, H.C., Ting, R.C., Kara, U.A., 1997. Direct PCR amplification and sequence analysis of extrachromosomal Plasmodium DNA from dried blood spots. Acta Trop. 68, 105–114.

Trager, W., Jensen, J.B., 1976. Human malaria parasites in continuous culture. Science 193, 673–675.

Vaidya, A.B., Akella, R., Suplick, K., 1989. Sequences similar to genes for two mitochondrial proteins and portions of ribosomal RNA in tandemly arrayed 6-kilobase-pair DNA of a malarial parasite. Mol. Biochem. Parasitol. 35, 97–107.

van den Hoff, M.J., Moorman, A.F., Lamers, W.H., 1992. Electroporation in 'intracellular' buffer increases cell survival. Nucleic Acids Res. 20, 2902.

van Dooren, G.G., Marti, M., Tonkin, C.J., Stimmler, L.M., Cowman, A.F., McFadden, G.I., 2005. Development of the endoplasmic reticulum, mitochondrion and apicoplast during the asexual life cycle of *Plasmodium falciparum*. Mol. Microbiol. 57, 405–419.

Vincent, R., Nadeau, D., 1983. A micromethod for the quantitation of cellular proteins in Percoll with the Coomassie brilliant blue dye-binding assay. Anal. Biochem. 135, 355–362.

Vollmer, M., Thomsen, N., Wiek, S., Seeber, F., 2001. Apicomplexan parasites possess distinct nuclear-encoded, but apicoplast-localized, plant-type ferredoxin-NADP$^+$ reductase and ferredoxin. J. Biol. Chem. 276, 5483–5490.

Wilson, R.J., Fry, M., Gardner, M.J., Feagin, J.E., Williamson, D.H., 1992. Subcellular fractionation of the two organelle DNAs of malaria parasites. Curr. Genet. 21, 405–408.

Wilson, R.J.M., Denny, P.W., Preiser, P.R., Rangachari, K., Roberts, K., Roy, A., Whyte, A., Strath, M., Moore, D.J., Moore, P.W., Williamson, D.H., 1996. Complete gene map of the plastid-like DNA of the malaria parasite *Plasmodium falciparum*. J. Mol. Biol. 261, 155–172.

Available online at www.sciencedirect.com
ScienceDirect
Parasitology International 56 (2007) 31–43
www.elsevier.com/locate/parint

The *Plasmodium falciparum* RhopH2 promoter and first 24 amino acids are sufficient to target proteins to the rhoptries

Ahmed Ghoneim [a], Osamu Kaneko [a], Takafumi Tsuboi [b,c], Motomi Torii [a,*]

[a] *Department of Molecular Parasitology, Ehime University Graduate School of Medicine, Shitsukawa, Toon, Ehime 791-0295, Japan*
[b] *Cell-Free Science and Technology Research Center, Ehime University, Matsuyama, Ehime 790-8577, Japan*
[c] *Venture Business Laboratory, Ehime University, Matsuyama, Ehime 790-8577, Japan*

Received 6 October 2006; received in revised form 29 October 2006; accepted 1 November 2006
Available online 15 December 2006

Abstract

The rhoptry secretory organelles of the malaria parasite, *Plasmodium falciparum*, contain a RhopH complex, which is composed of the proteins RhopH1, RhopH2, and RhopH3. RhopH1 is encoded by the *rhoph1/clag* multi-gene family, whereas RhopH2 and RhopH3 are encoded by single-copy genes. The precise function of the RhopH complex has not been identified, but it has been shown that the component proteins are involved in erythrocyte binding and perhaps participate in the formation of the parasitophorous vacuolar membrane. In this study, we have isolated *pfrhoph2* promoter plus the signal peptide encoding sequence and generated transgene expression constructs to evaluate a trafficking and the RhopH complex formation in transgenic *P. falciparum* parasite lines. Interestingly, we found that the N-terminal 24 amino acids of RhopH2, including signal peptide sequence, were sufficient to target GFP to the rhoptries under the *rhoph2* promoter. Because it was previously shown that the timing of the expression alone could not target proteins to the apical organelles, this targeting is likely mediated via a unique mechanism that is dependent on N-terminal 24 amino acids of RhopH2 early in the secretory pathway. The N-terminal one third of Clag3.1, which contains a distinct conserved domain with *Toxoplasma gondii* RON2, can not associate the RhopH complex as a GFP chimera, but a c-Myc-Clag3.1 chimera lacking the C-terminus successfully associates the RhopH complex indicating that cooperation of middle region is likely required but the C-terminus is not necessary.

Keywords: *Plasmodium falciparum*; Rhoptry; RhopH complex; Secretion; Protein targeting

1. Introduction

Plasmodium falciparum is the most potent and deadly species of human malaria parasites, and is responsible for several hundred millions infections and approximately 2 million deaths each year. The morbidity and mortality is exclusively due to blood stream burdens of the intra-erythrocytic stages of the parasite. The erythrocyte-invasive merozoite stages of the parasite use an elaborate apical complex apparatus in order to penetrate the host erythrocyte and establish an enclosing parasitophorous vacuole (PV). In this niche the parasite safely avoids immune surveillance, but acquires nutrients from the erythrocyte cytoplasm and across the erythrocyte surface membrane, for growth, rapid replication, and eventual lysis of the host cell to release merozoites. The merozoite apical secretory apparatus comprises three organelles: the rhoptries, micronemes, and the dense granules, the contents of which play a predominant role in the invasion process and establishment of the PV.

Following the attachment of merozoites to the erythrocyte surface, rhoptry organelles discharge their contents onto the erythrocyte membrane [1]. The rhoptries disappear after erythrocyte invasion and thus are formed *de novo* with each erythrocytic cycle. Rhoptry formation occurs late in the erythrocytic stages of the parasite, at around 40 h after invasion [2]. Elucidation of rhoptry biogenesis of malaria parasites has been hindered by the lack of early organelle markers, and most of our

Abbreviations: aa, amino acid; c-Myc, cellular homologue of myelocytomatosis virus 29 oncogene; *clag*, cytoadherence-linked asexual gene; ER, endoplasmic reticulum; GFP, green fluorescent protein; PBS, phosphate buffered saline; PCR, polymerase chain reaction; PV, parasitophorous vacuole.

* Corresponding author. Tel.: +81 89 960 5285; fax: +81 89 960 5287.
E-mail address: torii@m.ehime-u.ac.jp (M. Torii).

1383-5769/$ - see front matter © 2006 Elsevier Ireland Ltd. All rights reserved.
doi:10.1016/j.parint.2006.11.001

knowledge stems from microscopic examinations of cellular ultrastructure. These studies suggest that rhoptry biogenesis follows the secretory pathway route, and rhoptry organelles are formed by sequential fusion of post-Golgi vesicles [3,4]; although it remains unclear why particular vesicles are selected in the formation of rhoptries [5].

Several merozoite rhoptry components have been identified, including the high molecular mass RhopH complex which consists of three non-covalently associated proteins: RhopH1, RhopH2, and RhopH3 [6–9]. RhopH1 is encoded by three members of the *rhoph1/clag* family, namely, *clag2*, *clag3.1*, and *clag9* [10–12]. The RhopH complex is conserved across *Plasmodium* species and is localized to the rhoptries of mature merozoites, and subsequently retained in the newly formed ring stage parasites following erythrocyte invasion [13]. The function of the complex has not been determined, although it is proposed that the protein complex is involved in erythrocyte binding during or after invasion [14,15], and perhaps participates in the formation of the parasitophorous vacuolar membrane (PVM) [11,13]. It has also recently been proposed that the RhopH complex is a candidate translocon which mediates protein translocation through the PV to the host cell cytoplasm or its surface [16], based upon the finding that in later stages, newly synthesized RhopH2 and RAP3 can also be found in association with Maurer's clefts [17].

Several studies [18–21] have reported that the classical endoplasmic reticulum (ER)-type signal sequence is sufficient for protein recruitment into the secretory pathway within the parasite, and that the PV is the default transit destination for these proteins. These results also imply that targeting to other organelles must require a secondary signal and sorting system. For example, it was recently shown that a Pexel/VTS motif adjacent the signal peptide is required for protein export beyond the PV into the erythrocyte cytoplasm [22,23]. As a second example, apicoplast targeted proteins possess a transit peptide, in addition to the classical ER-signal peptide, for import into the apicoplast [18].

All *Plasmodium* rhoptry proteins analyzed to date contain hydrophobic N-terminal signal peptides, suggesting export via the classical secretory pathway, but thus far no studies have addressed the mechanism of their trafficking and targeting to rhoptries. In this report we exploited the ability to follow the expression of fluorescent proteins in living cells to investigate the signals responsible for the targeting of the RhopH complex proteins to their destination and to explore if the N-terminus of Clag3.1 is responsible for the incorporation of this protein into the complex. Expressing these proteins as chimeras with the green fluorescent protein (GFP) enabled us to visualize rhoptry biogenesis in *P. falciparum*.

2. Materials and methods

2.1. Plasmid constructs

2.1.1. Construction of a basic plasmid vector with a rhoptry gene promoter

The plasmid pHH1 [24] was restriction digested with *Eco*RI and *Hin*dIII to remove the *calmodulin* 5′ untranslated region (UTR), the human *dihydrofolate reductase* (*hdhfr*) ORF, and the *histidine rich protein 3* 3′ UTR. A linker oligonucleotide (AGCTTCCCGGGATCCGTCGACGAATT) that contains the restriction sites *Sma*I, *Bam*HI, and *Sal*I was added to produce the plasmid pH86DT. The *heat shock protein* (*hsp*) *86* 5′ UTR was removed by digesting this plasmid with *Xho*I and *Sma*I and the cohesive end was filled-in using *Taq* DNA polymerase and followed by self-ligation to produce the plasmid pPbDT3U. The regenerated *Xho*I site was then destroyed by *Xho*I digestion and filling in the ends to produce the plasmid pPbDT3UΔX.

To clone a rhoptry gene promoter, *pfrhoph2* 5′ UTR plus the signal peptide encoding sequence was PCR-amplified from 3D7 strain genomic DNA (gDNA) using the forward primer ATACCCCTCGAGTTTTTTGAAAAATATAAAATCGTGC (with *Xho*I site underlined) and the reverse primer ATACCCCTCGAG*ATCCTCTTCTGAGATGAGTTTTTGTT*-CACTAGTATTCAATTCTAATCCATACAAG which adds *c-myc* epitope sequence (italic) flanked by *Xho*I and *Spe*I sites (underlined). The amplicon included 1027 bp upstream to the start codon and a downstream 69 bp. This amplicon was subcloned into pGEM-T Easy plasmid (Promega, Madison, WI) and the *Xho*I-restriction fragment was ligated into *Sal*I site of pPbDT3UΔX to produce the plasmid pRDT.

pHRPGFPm2 [25] was obtained from K. Haldar through the Malaria Research and Reference Reagent Resource Center, Division of Microbiology and Infectious Diseases, NIAID, NIH and used to amplify GFP with the forward primer ATTGGAAGATCTCTCGAGCCCGGGGCTAGCTC-TAGAAAAGGAGAAGAACTTTTCACTGGAG (with *Bgl*II, *Xho*I, *Sma*I, *Nhe*I, and *Xba*I sites underlined) and the reverse primer ATTGGAAGATCTCTAGTCGACTTTGTA-TAGTTCATCCATGCCA (with *Bgl*II and *Sal*I sites underlined). The amplified DNA fragment was subcloned into pGEM-T Easy, then the *Bgl*II-restriction fragment was ligated into *Bam*HI site of pRDT to produce the plasmid pRGDT (Fig. 1). pRGDT contains *pfrhoph2* 5′ UTR, followed by *pfrhoph2* signal peptide encoding sequence, *Spe*I, *c-myc* tag sequence, multiple cloning site, *gfp* ORF, and *P. berghei* DHFR-TS 3′ UTR (PbDT3′UTR).

The *att*B1 linker (CTAGACAAGTTTGTACAAAAAAG-CAGGCTCTAG) and *att*B2 linker (GGCCACCCAG-CTTTCTTGTACAAAGTGGTGGCC) were inserted into *Avr*II and *Not*I sites, respectively, to convert the plasmid pRGDT into *attB* expression clone (pRGDT-B12), which is ready for the Gateway BP recombination reaction (Invitrogen, Carlsbad, CA) (Fig. 1A).

2.1.2. Construction of the plasmid expressing RhopH2-Myc-Clag3.1$_{(24–483)}$-GFP chimeric protein

To express the N-terminal one third of PfClag3.1 as a chimeric protein fused with c-Myc to its N-terminus and GFP to its C-terminus, we used a pGEM-T Easy clone containing a part of *clag3.1* coding sequence of HB3 strain as a template to amplify the 5′ region encoding the first N-terminal 460 amino acids of the protein after the expected cleavage site of its signal peptide (Fig. 2) using the forward primer

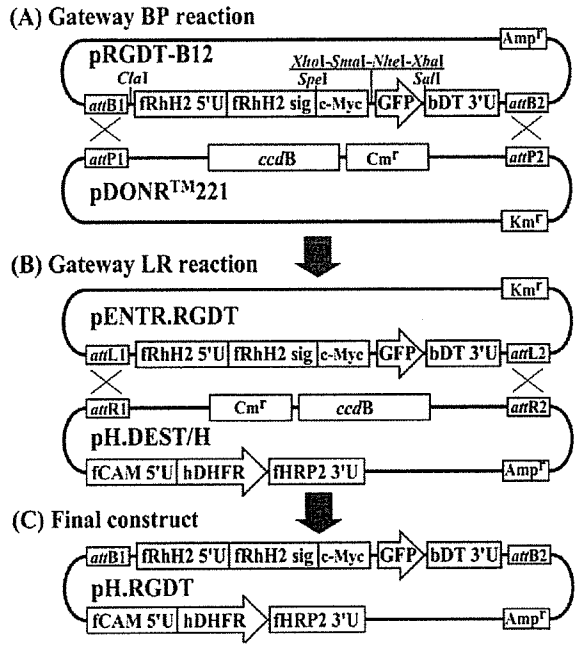

Fig. 1. A schematic diagram of some of the constructs produced in this study. (A) A novel transfection plasmid (pRGDT-B12) with *Plasmodium falciparum pfrhoph2* promoter. Protein of interest would be expressed as a fusion protein with c-Myc tag at its N-terminus and/or GFP at its C-terminus. Several unique restriction sites are available for one-step ligation on both sides of *c-myc* and *gfp* (detail of the one-step ligation is described in the Materials and methods section). The plasmid also contains the Gateway *att*B recombination sites and thus ready to be manipulated by the Invitrogen Gateway technology. This *att*B expression clone was subjected to BP Gateway recombination reaction with the donor vector pDONR™221 to produce the entry clone pENTR.RGDT with *attL* sites (B), which was then subjected to LR recombination reaction with the destination vector pH.DEST/H containing the *att*R sites and the selectable marker *hdhfr* to produce the final transfection construct pH.RGDT (C). pH.RGDT contains the both of the *rhoph2-myc-gfp* expression cassette and the selectable marker *hdhfr* expression cassette.

GTCGACTGTTCAATAAATGAAAATCAAAATGAAAATG (with *Sal*I site underlined) and the reverse primer GTCGACAGATCTTGTATCATAATTTAAAAGTCCAG (with *Sal*I site underlined). The amplicon was subcloned into pGEM-T Easy, and the *Sal*I-restriction fragment was ligated into *Xho*I site of pRGDT-B12 by one-step ligation to produce the plasmid pRGDT-Clag3.1A-B12 (Fig. 1). One-step ligation was performed in a 10 μl reaction mixture (pH 7.9), containing 100 ng of the *Sal*I-restriction fragment, 100 ng of pRGDT-B12, 10 mM Tris–HCl, 10 mM $MgCl_2$, 50 mM NaCl, 1 mM dithiothreitol, 10 ng of BSA, 1 mM ATP, 7 units of *Xho*I, and 200 units of T4 DNA ligase. The reaction mixture was incubated at 16 °C overnight and after inactivation of T4 DNA ligase at 65 °C for 10 min, this mixture was further incubated at 37 °C for several hours for complete digestion of the remaining pRGDT-B12 and transformed into *Escherichia coli* according to the standard protocol. The recombination between *Sal*I-restriction fragment and the *Xho*I-digested plasmid kills *Xho*I site thus rendering the recombined plasmid resistant to digestion whereas the unrecombined plasmid will be easily digested. This enriches the reaction mixture with recombined plasmids.

2.1.3. Construction of the plasmid encoding RhopH2-Myc-Clag3.1Full-GFP chimeric protein

To produce the full length of PfClag3.1 fused with c-Myc to its N-terminus and GFP to its C-terminus, we used pGEM-T Easy clones containing the sequences encoding the middle and C-terminal parts of Clag 3.1 as templates. The middle region of

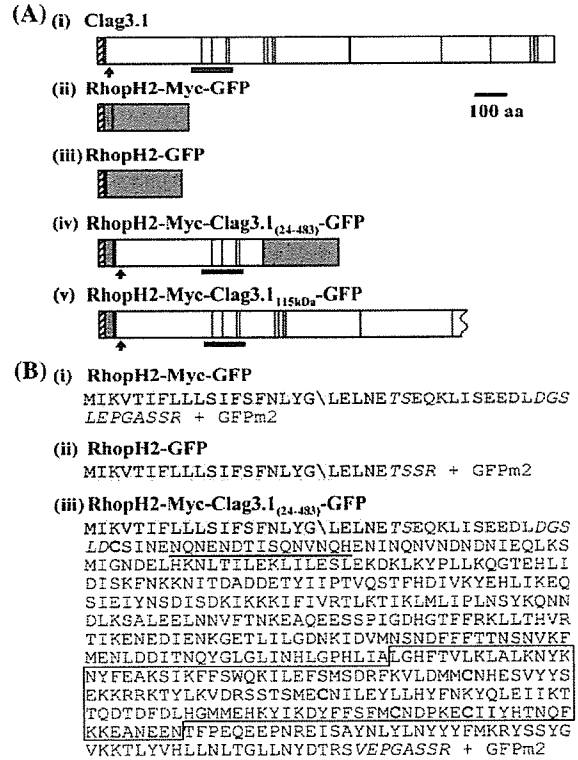

Fig. 2. (A) Structure of the chimeric proteins expressed in transgenic *Plasmodium falciparum*. (i) A schematic diagram of the domain structure of the endogenous Clag3.1. Red vertical lines indicate Cys residues conserved throughout the RhopH1/Clag family and black lines indicate the partially conserved ones. Striped box indicates the putative signal peptide sequence. (ii) RhopH2-Myc-GFP chimeric protein expressed from the transfection construct pH.RGDT. This protein contains the putative signal peptide sequence of PfRhopH2 plus c-Myc and GFP. Blue box represents c-Myc tag and green box represents GFP. (iii) RhopH2-GFP chimeric protein expressed from the construct pH.RGDTΔMyc. (iv) RhopH2-Myc-Clag3.1$_{(24\ 483)}$-GFP chimeric protein expressed from the construct pH.RGDT-Clag3.1A. This protein contains the putative signal peptide sequence of PfRhopH2 and the amino acids 23–484 of Clag3.1 fused to c-Myc at its N-terminus and GFP at the C-terminus. (v) RhopH2-Myc-Clag3.1$_{115\ kDa}$ which represents a truncated chimeric protein expressed from the construct pH.RGDT-Clag3.1Full. In addition to the putative signal peptide sequence of PfRhopH2 and c-Myc tag at its N-terminus, this protein is estimated to comprise N-terminal 115 kDa of Clag3.1 after the signal peptide cleavage site. Arrows under the schema indicate the target region of rabbit anti-Clag3.1 serum. (B) Amino acid sequence of the GFP chimeric proteins expressed from pH.RGDT (i), pH.RGDTΔMyc (ii), and pH.RGDT-Clag3.1A (iii). Amino acid sequence shaded with gray color represents the putative signal sequence plus 5 amino acids from PfRhopH2 with the back slash indicating the putative cleavage site between Gly_{19} and Leu_{20} as predicted by SignalP 3.0. c-Myc tag sequence is blue in bold, the amino acids introduced for cloning purpose are shown in italic, and the conserved Cys residues are red in bold. Amino acid sequence recognized by rabbit anti-Clag3.1 serum is underlined. Sequence harboring strong homology with PF14_0495 was boxed and indicated in panel Ai with thick bars under the schema. (For interpretation of the references to colour in this figure legend, the reader is referred to the web version of this article.)

clag3.1 was amplified with the forward primer TCGCGGATCC-TATGTGACATCACTTTATTTACCAGG (with *Bam*HI site underlined) and the reverse primer TCGCGGATCCACATAT-CATACATTTTGGATGCTAGC (with *Bam*HI site underlined). The amplicon was subcloned into pGEM-T Easy, sequenced and the *Bam*HI-restriction fragment was ligated by one-step ligation into the endogenous *Bgl*II site that exists in the 3′ end of *clag3.1* gene in the plasmid pRGDT-Clag3.1A-B12 to produce the plasmid pRGDT-Clag3.1AB-B12. The sequence encoding the C-terminal region of Clag3.1 was amplified from the respective pGEM-T Easy clone with the forward primer CTAGTCTAGAATCCAAAATGTATGATATGTTAAATTA-TAA (with *Xba*I site underlined) and the reverse primer CTAGTCTAGAGTGAAATCGTGCGATCATTAATTCATTG (with *Xba*I site underlined). The amplicon was subcloned into pGEM-T Easy, sequenced, and the *Xba*I-restriction fragment was ligated into the endogenous *Nhe*I site that exists in the 3′ end of *clag3.1* gene in the plasmid pRGDT-Clag3.1AB-B12 to produce the plasmid pRGDT-Clag3.1Full-B12.

2.1.4. Preparation of destination vector

pHH1 was digested with *Hpa*I and *Not*I to remove the *hsp86* 5′ UTR and *PbDT* 3′ UTR and after blunting the *Not*I-cohesive end, the Gateway reading frame cassette B containing the *att*R recombination sites (Invitrogen) was ligated to produce the destination vector pH.DEST/H with the *att*R1 recombination site in a head-to-head orientation with human *dhfr* cassette (Fig. 1B).

2.1.5. Gateway recombination reactions

pRGDT-B12, pRGDT-Clag3.1A-B12, and pRGDT-Clag3.1-Full-B12 were subjected to BP recombination reaction with the donor vector pDONR™221 (Invitrogen) according to the manufacturer's instructions to produce the corresponding entry clones pENTR.RGDT, pENTR.RGDT-Clag3.1A, and pENTR.RGDT-Clag3.1Full (Fig. 1A). Then, these entry plasmids were subjected to LR recombination reaction according to the manufacturer's instructions (Invitrogen) with pH.DEST/H to produce the final stable transfection vectors pH.RGDT, pH.RGDT-Clag3.1A, and pH.RGDT-Clag3.1Full (Fig. 1B). Each vector contains 2 expression cassettes in a head-to-head orientation; the gene of interest cassette driven under the control *pfrhoph2* promoter and the human *dhfr* driven under the control of *pfcalmodulin* promoter.

2.1.6. Construction of the plasmid expressing RhopH2-GFP chimeric protein

To express GFP appended to RhopH2 signal peptide and a minimal peptide spacer (Fig. 2), the sequence encoding c-Myc tag and the multiple cloning site were removed by digesting the final transfection vector pH.RGDT directly with *Spe*I and *Nhe*I and self-ligation to produce the vector pH.RGDTΔMyc.

2.2. Parasite culture and transfection

The Dd2 strain of *P. falciparum* was grown *in vitro* essentially under the standard conditions [26]. Parasite transfection was carried out as described previously [27]. Briefly, erythrocytes were washed with incomplete cytomix and loaded with 100 μg of the desired transfection construct using the electroporation system (Bio-Rad, Hercules, CA). Late parasite stages were then inoculated into the plasmid-loaded erythrocytes and parasites were allowed to invade and grow for 3 days before applying the drug WR99210 at 10 nM concentration. Transfected parasites were collected as late schizonts for protein analysis after two rounds of 5% sorbitol treatment. For time course protein analysis, parasites were synchronized using a MACS Type-D depletion column in conjunction with a SuperMACS II magnetic separator (Miltenyi Biotec GmbH, Germany) [28,29]. Culture was passed through the column and schizonts were collected, washed, and inoculated into new uninfected erythrocytes, allowed for rupture and invasion. Four hours later, the culture was passed again through the column and the remaining unruptured schizont-infected erythrocytes were removed and ring stages were allowed to complete a cycle. Equal aliquots of culture were harvested at 0 h and every 8 h thereafter.

2.3. Antibodies

Antibodies used for Western blot analysis and immunoprecipitation were: mouse anti-RhopH2 monoclonal antibody (mAb) 4E10 [13], mouse anti-GFP mAb (GF200; Nacalai, Japan), mouse anti-c-Myc mAb (9E10; Sigma, St. Louis, MO), rabbit anti-Clag3.1 serum, and mouse anti-Clag9 serum [12].

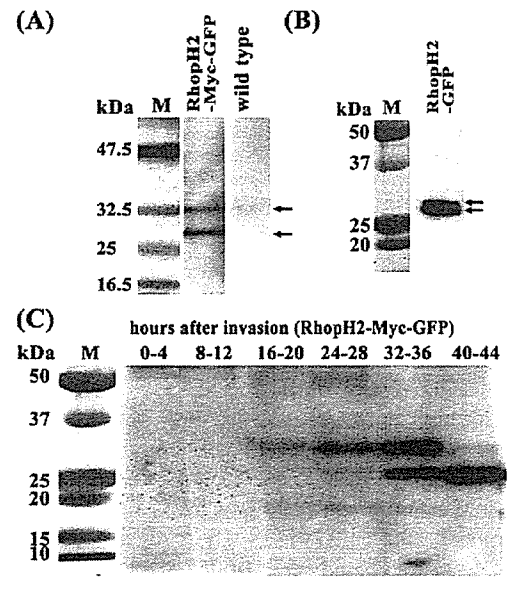

Fig. 3. Western blot analysis of RhopH2-Myc-GFP and RhopH2-GFP chimeric proteins. Proteins were extracted from schizont stage pH.RGDT-transfected parasites and wild type parasites (A) or pH.RGDTΔMyc-transfected parasites (B), and then visualized with anti-GFP mAb on the PVDF membrane after SDS-PAGE. Two bands (32 and 29 kDa; arrows) seen in panel A and 2 overlapping bands (~29 and 27 kDa; arrows) seen in panel B appear to represent the premature and processed forms of the chimeric protein, respectively. (C) Time course of the RhopH2-Myc-GFP chimeric protein expression in the parasites transfected with pH.RGDT over 44 h. Parasites were synchronized to 4 h window, and then harvested every 8 h after erythrocyte invasion for 1 complete cycle.

Antibodies used for immunofluorescence assay were: rabbit anti-Clag9 serum [11], rabbit anti-AMA1 serum (a kind gift from C. Long) and anti-GFP mAb (JL-8; BD living colors).

2.4. Western blot analysis

Parasite proteins were extracted by repeated freeze–thaw cycles, dissolved in 1× SDS-PAGE loading buffer and run on 5–20% polyacrylamide gel (ATTO, Japan) after incubation at 100 °C for 3 min. Proteins were blotted onto a 0.22 μm PVDF membrane (Bio-Rad) and immunostained with the specific primary antibodies or antisera followed by horseradish peroxidase-conjugated secondary antibody staining (Biosource Int., Camarillo, CA) and visualized with ECL Plus (Amersham Biosciences, UK) on RX-U film (Fuji, Japan).

2.5. Immunoprecipitation analysis

Immunoprecipitation was carried out as described previously [30]. Briefly, proteins were extracted from late schizont parasite pellets by repeated freeze–thaw cycles in PBS containing a cocktail of proteinase inhibitors. Supernatants (100 μl) were pre-incubated for 1 h at 4 °C with 40 μl of 50% protein G-conjugated beads (GammaBind Plus Sepharose; Amersham Biosciences) in NETT buffer (50 mM Tris–HCl, 0.15 M NaCl, 1 mM EDTA, and 0.5% Triton X-100) supplemented with 0.5% BSA (fraction V; Sigma). Recovered supernatants were incubated with rabbit anti-PfRhopH2 serum [7] or mouse anti-c-Myc mAb (9E10) with gentle rotation for 2 h at 4 °C and then 40 μl of 50% protein G-conjugated beads were added. After 1 h incubation at 4 °C, the beads were washed once with NETT-0.5% BSA, once with NETT, once with high-salt NETT (0.5 M NaCl), once with NETT, and once with low-salt NETT (0.05 M NaCl and 0.17% Triton X-100). Finally, proteins were extracted from the protein G-conjugated beads by incubation with SDS-PAGE loading buffer at 100 °C for 3 min. Supernatants were collected and stored at −70 °C until next day for Western blot analysis.

2.6. Immunofluorescence assay and microscopy

For GFP imaging, small aliquots of parasite culture were washed with PBS, incubated in PBS containing 4′, 6-diamidino-2-phenylindole (DAPI) for 5 min and then mounted without further treatment. Parasites expressing GFP were imaged using a fluorescence microscope (BX50; Olympus, Japan) and digital camera (IM500; Leica, Germany). Immunofluorescence assay was performed in the same way as described previously [12]. Briefly, schizont-rich infected erythrocytes were smeared on glass slides and stored at −80 °C until use. Later, smears were fixed in ice-cold acetone, pre-incubated with PBS containing 5% non-fat milk at 37 °C for 30 min and reacted with the desired primary antibody at 37 °C for 1 h. Smears were then washed with PBS and reacted with fluorescein isothiocyanate (FITC)-conjugated goat anti-(mouse IgG and IgM) secondary antibody (Biosource Int.) and Alexa546-conjugated

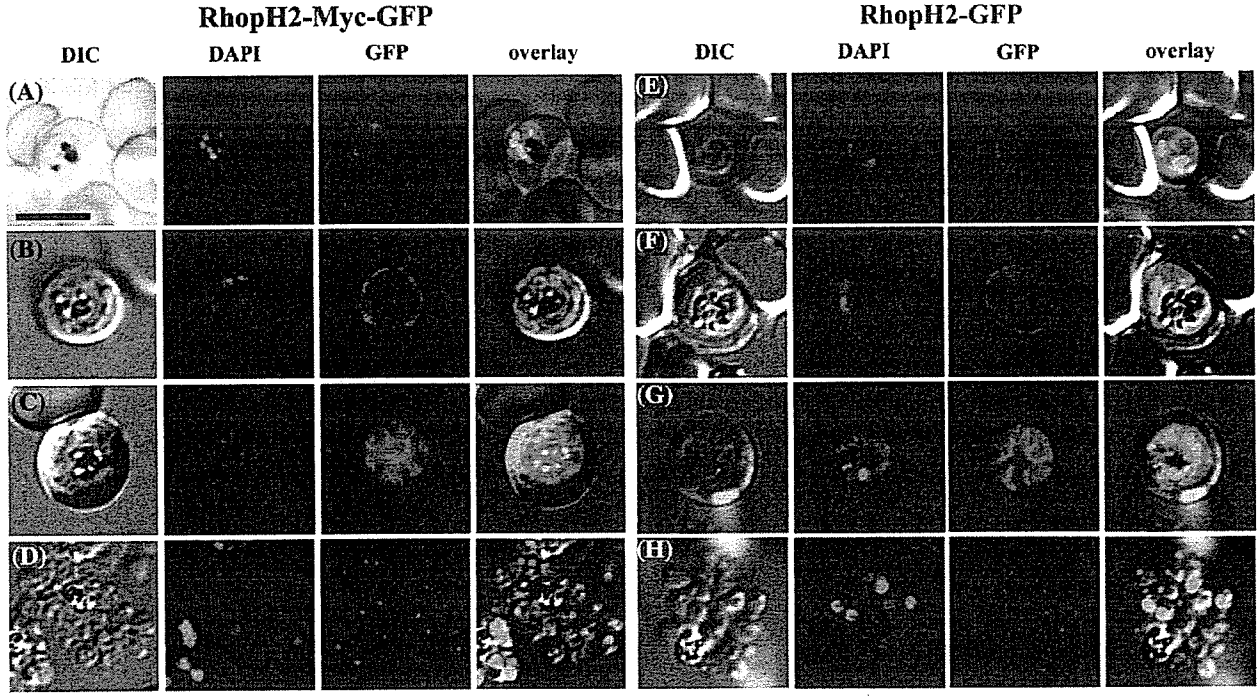

Fig. 4. Similar trafficking and subcellular localization of RhopH2-Myc-GFP (A–D) and RhopH2-GFP (E–H) chimeric proteins during late developmental stages of parasite growth. Images were collected from live parasites. (A and E) Early schizont stages showing almost even fluorescence signal in the cytoplasm and probably the parasitophorous vacuole. (B and F) Further developed schizonts showing accumulation of the chimeric proteins around the parasites. (C and G) Later schizont stages showing fluorescence surrounding individual merozoites. Fluorescent vesicles can be seen; probably representing premature rhoptries. (D and H) Segmented schizonts showing concentrated fluorescence signal at the apical end of the formed merozoites. Nuclei were stained with DAPI. Scale bar represents 5 μm.

goat anti-rabbit-IgG (H+L) secondary antibody (highly cross-adsorbed; Molecular Probes, Eugene, OR) at 37 °C for 30 min. Images were captured as described above. Nuclear staining was performed using DAPI, the slides were mounted in ProLong antifade reagent (Molecular Probes), and images were processed using Adobe Photoshop software.

3. Results

3.1. Construction of a novel transfection vector with a rhoptry gene promoter

To study the protein trafficking of rhoptry proteins we constructed a vector, pRGDT-B12, which expresses proteins of interest fused to the RhopH2 signal peptide sequence and under the control of the rhoptry gene *pfrhoph2* promoter. The signal peptide sequence of the expressed fusion proteins is predicted to be cleaved between Gly_{19} and Leu_{20} (Fig. 2). As a mean to determine the cellular localization, the expressed proteins contain a c-Myc epitope downstream of the signal peptide and GFP at their C-terminus. The c-Myc epitope and GFP are both flanked by unique restriction sites for manipulation such that either can be removed from the expressed fusion proteins. The multiple unique restriction sites (*Xho*I, *Sma*I, *Nhe*I, and *Xba*I) between the c-Myc tag and GFP allow for a convenient one-step ligation reaction that does not require pre-digestion of the plasmid backbone. Variable restriction-fragments can be ligated into one restriction site (e.g. *Avr*II, *Spe*I, or *Xba*I-restriction fragments can be ligated into *Nhe*I site) with similar procedure to the ligation of *Sal*I-restriction fragment into *Xho*I site as used to generate pRGDT-Clag3.1A-B12 (see Material and methods). All components described above in pRGDT-B12 were flanked by the *att*B1 and *att*B2 Gateway recombination sites making it ready to recombine with the desired destination vector possessing a suitable selectable marker according to the Gateway technology. pRGDT-B12 with the carefully designed multiple cloning site provides more flexibility than the entry vector (pENTR.RGDT).

3.2. Characterization of the pfrhoph2 promoter

To confirm the ability of the *pfrhoph2* promoter to drive episomal expression of inserted gene sequences, we transfected *P. falciparum* with the plasmid pH.RGDT and generated a parasite line retaining the plasmid as a stable episome. Western blot analysis of late schizont stage transformants using anti-GFP serum showed two clear bands at 32 kDa and 29 kDa (Fig. 3A) that are specific to transfected parasites. The 32-kDa band corresponds to the expected size of the unprocessed RhopH2-Myc-GFP chimeric protein expressed from pH.RGDT, whereas the 29-kDa band is consistent with the size expected for the mature protein after cleavage of the signal peptide sequence (Fig. 2A).

To evaluate the timing of protein expression under the *pfrhoph2* promoter, the transfected parasites were synchronized using a MACS apparatus and the 4 h-window parasites were collected every 8 h for Western blot analysis (Fig. 3C). Proteins collected at the ring stages (0–4 and 8–12 h) did not show any signal with anti-GFP serum. A single faint 32-kDa band corresponding to the size of the unprocessed protein form was detected from early trophozoite stage (16–20 h). The amount of the unprocessed chimeric protein gradually increased until it reached a peak at schizont stage (32–36 h), then it ceased dramatically in the mature schizont stage (40–44 h). Another

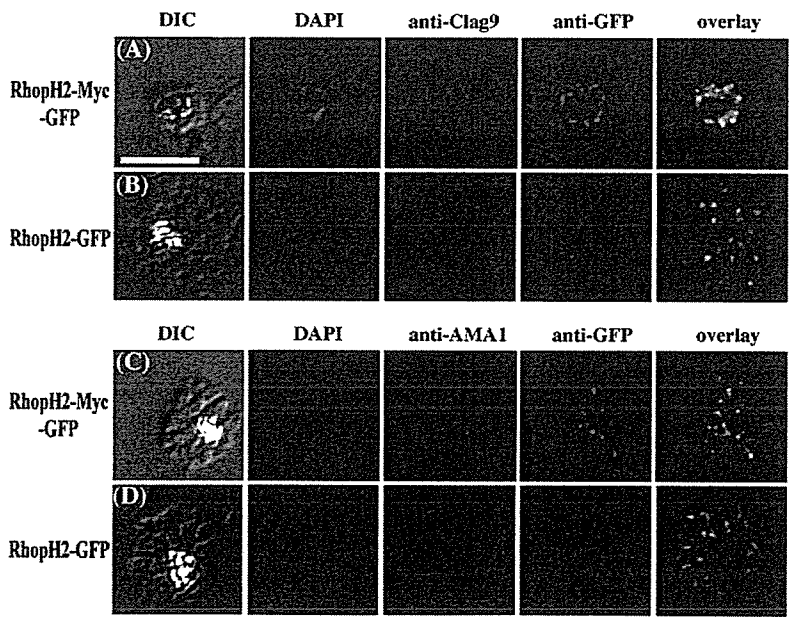

Fig. 5. Co-localization of GFP chimeric proteins with the rhoptry protein Clag9 but not with the microneme protein AMA1. (A and C) Late schizonts expressing RhopH2-Myc-GFP chimeric protein. (B and D) Late schizonts expressing RhopH2-GFP chimeric protein. Air-dried segmented schizonts were fixed with acetone and reacted with anti-GFP mAb, and rabbit anti-Clag9 serum or rabbit anti-AMA1 serum. Nuclei were stained with DAPI. Scale bar represents 5 μm.

faint but discrete 29-kDa band corresponding to the size of the mature protein form was detected in late trophozoite stage (24–28 h). The amount of the mature form gradually increased until the end of the asexual life cycle (40–44 h) when its peak expression was observed. The expression pattern shown here may suggest a post-translational recruitment of the fusion protein into the ER. Although expression of the chimeric protein here seems to be slightly earlier when compared to the transcription of native *rhoph2*, which was detected after 30 h post-invasion [11], our results show that RhopH2-Myc-GFP chimera was correctly processed and showed peak expression at the mature schizont stage. This validates the use of *pfrhoph2* promoter in studying the proteins that are expressed in late schizont stage.

3.3. The RhopH2 promoter and first 24 amino acids are sufficient to target proteins to the rhoptries

Transgenic *P. faciparum* parasite line that express RhopH2-Myc-GFP chimeric protein showed strong green fluorescence during the schizont stage of the parasite growth. The expressed chimeric protein consists of the ER signal peptide sequence plus a short linker sequence and c-Myc tag and GFP (Fig. 2Bi). No fluorescence signal was detected in ring or trophozoite stages, whereas early schizont stage parasites showed uniform green fluorescence throughout the cell and maximal expression at the periphery of the parasite (Fig. 4A). This fluorescence pattern is consistent with chimeric protein localization within the parasite cytoplasm and likely the PV. As the intra-erythrocytic parasites matured (Fig. 4B), the fluorescence signal increased in specific marginal areas. In mature parasites a segmented fluorescence pattern surrounding the individual merozoites was observed, which again is consistent with trafficking of the proteins to the PV (Fig. 4C). Some vesicles can be seen within individual immature merozoites, which might be immature rhoptry vesicles. In the segmented schizonts, the fluorescence signal was clearly localized at the apical end and the fluorescence surrounding the merozoites disappeared, probably because the erythrocyte and PV membranes were partly ruptured (Fig. 4D). This pattern was repeatedly observed with no obvious differences despite an extensive investigation of a large number of schizonts.

Foth et al. [31] has shown that targeting proteins to the apicoplast is influenced by the acidic amino acids downstream to the signal peptide. To evaluate whether this is the case, we generated *P. falciparum* parasite line expressing a chimeric protein RhopH2-GFP by transfecting with pH.RGDTΔMyc. This chimeric protein lacks c-Myc tag and contains only 9 amino acids (LELNETSSR) between the RhopH2 signal peptide and GFP (Fig. 2Bii). Thus, this chimeric protein lacks 6 out of the 8 acidic amino acids existing in RhopH2-Myc-GFP chimera and, in total, 7 charged amino acids out of 10 were removed. Western blot analysis of the RhopH2-GFP chimeric protein revealed 2 overlapping bands (~29 and 27 kDa) that appear to represent the premature and processed forms of the chimeric protein, respectively (Fig. 3B). Trafficking pattern of RhopH2-GFP during the erythrocytic cycle was identical to that of RhopH2-Myc-GFP (Fig. 5E–H). These data indicate that both GFP chimeric proteins were similarly expressed in the cytoplasm at early schizont stage; and later, during merozoite formation, these proteins were translocated to the apical end of the newly formed merozoites in the late schizont stage parasite, suggesting that these proteins are targeted to a specific apical organelle.

To evaluate the subcellular localization of GFP-chimeric proteins in late schizont stages, we performed a double immunofluorescence staining assay on mature segmented schizont stage parasites using an anti-GFP mAb plus rabbit anti-Clag9 serum or rabbit anti-AMA1 serum. For both parasite lines, the GFP-chimeric proteins were co-localized with Clag9, an authentic rhoptry protein, but were not co-localized with AMA1, an authentic microneme protein. This suggests that both GFP-chimeric proteins were successfully targeted to the rhoptries, but not to the micronemes. Thus, the first 24 amino acids of RhopH2 including signal peptide sequence is sufficient to target proteins to the rhoptries under the *rhoph2* promoter sequence.

3.4. Expression of RhopH2-Myc-Clag3.1$_{(24–483)}$-GFP chimeric protein

The RhopH1/Clag protein family members possess an N-terminal domain that contains 4 conserved Cys residues. A TBLASTN search of the *P. falciparum* genome sequence

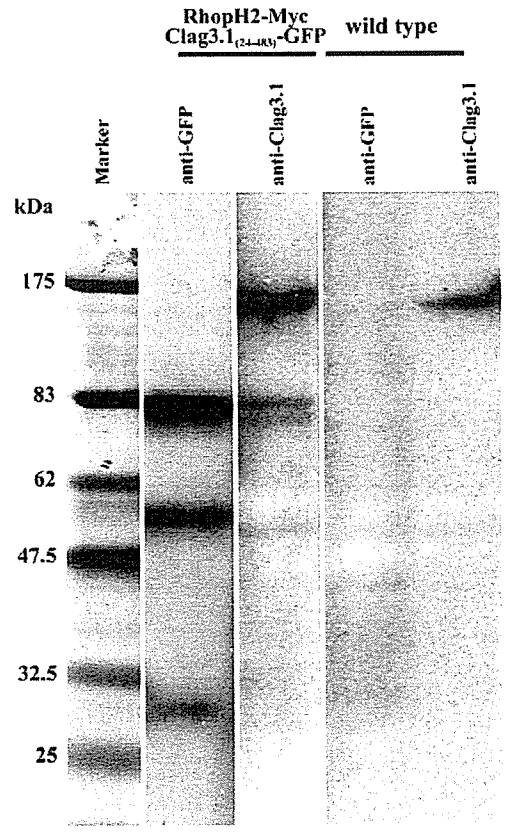

Fig. 6. Western blot analysis of the RhopH2-Myc-Clag3.1$_{(24\ 483)}$-GFP chimeric protein. Proteins were extracted from schizont stage pH.RGDT-Glag3.1A-transfected parasites and wild type parasites, and then visualized with anti-GFP mAb or anti-Clag3.1 serum on the PVDF membrane after SDS-PAGE.

database, using the Clag2 amino acid sequence as a query, identifies this domain within an additional ORF (PF14_0495 in PlasmoDB) that is most similar to the N-terminus of Clag2 (Fig.2) and represents a discrete domain of unknown function. Based on this domain prediction and because the Clag3.1 domain responsible for associating the other components of the RhopH complex is unknown, we selected the N-terminal one third of Clag3.1 (Fig. 2) to evaluate if this region is responsible for its involvement in the high molecular weight RhopH complex. To this end, we generated the transfection vector pH. RGDT-Clag3.1A that would express Clag3.1 (aa 24–483) as a chimeric protein with PfRhopH2 signal peptide and c-Myc tag at its N-terminus and GFP at its C-terminus (RhopH2-Myc-Clag3.1$_{(24–483)}$-GFP; Fig. 2Aiv). This construct was used to generate a parasite line retaining the plasmid as a stable episome.

The integrity of the expressed chimeric protein was confirmed by Western blot analysis of transfected parasite extracts using mouse anti-GFP mAb and rabbit anti-Clag3.1 serum that recognizes aa 29–43 of Clag3.1. As shown in Fig. 6, anti-GFP mAb recognizes three bands with sizes of approximately 82, 54, and 28 kDa. In contrast, the anti-Clag3.1 serum identified three bands having molecular weights of roughly 153,

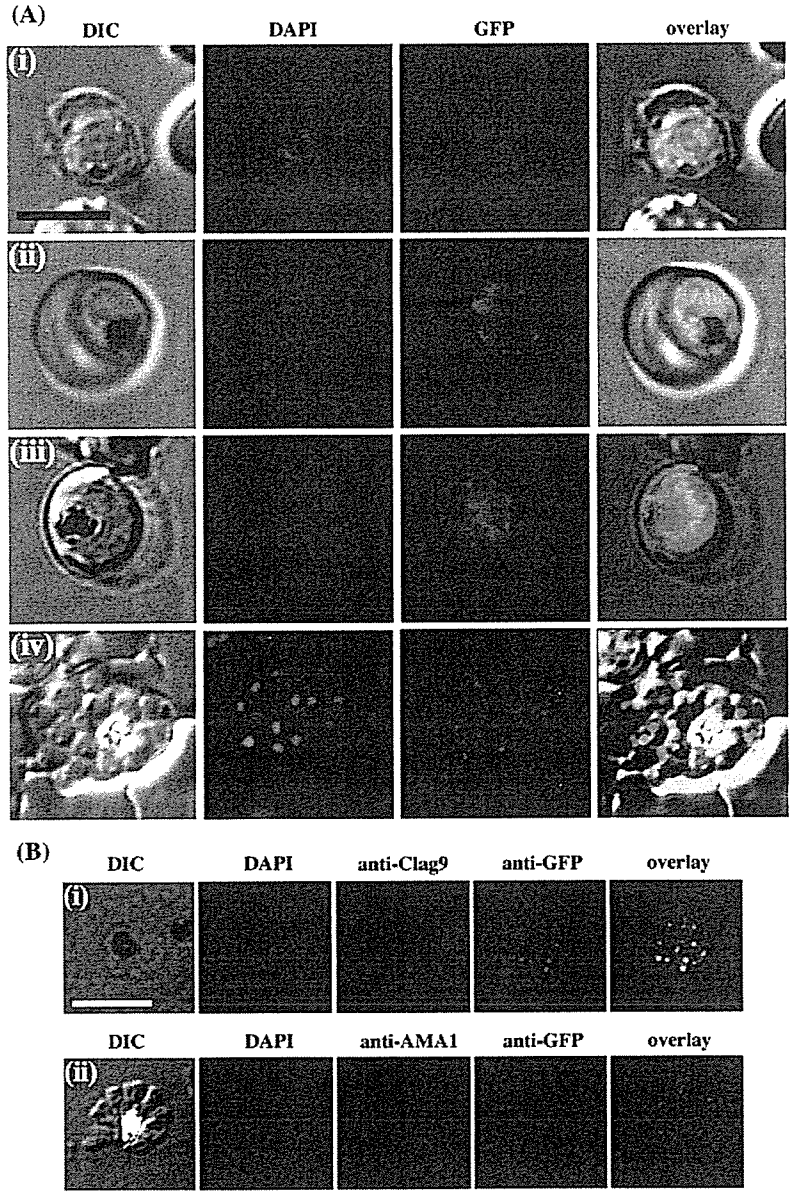

Fig. 7. Characterization of the parasites expressing the RhopH2-Myc-Clag3.1$_{(24\ 483)}$-GFP chimeric protein. (A) Trafficking and subcellular localization of RhopH2-Myc-Clag3.1$_{(24\ 483)}$-GFP chimeric protein during the late stages of parasite growth is identical to those of RhopH2-Myc-GFP and RhopH2-GFP chimeric proteins shown in Fig. 4. Images from early schizont stage (i), further developed schizont (ii), later schizont stage (iii), and segmented schizont (iv) are shown. Nuclei were stained with DAPI. (B) The RhopH2-Myc-Clag3.1$_{(24\ 483)}$-GFP chimeric protein co-localized with the rhoptry protein Clag9 (i), but not with the microneme protein AMA1 (ii). Scale bar represents 5 μm.

82, and 80 kDa. The band in common with the two antisera, of 80–82 kDa molecular weight, is consistent with the expected size of the unprocessed and mature forms of the chimeric protein (Fig. 2Biii). Thus, the chimeric protein possessing Clag3.1 N-terminus appears to be correctly targeted to the ER, and the signal peptide is cleaved. The 54-kDa band detected with anti-GFP mAb is likely a truncated form of the chimeric protein and the 28-kDa band corresponds to the size of a GFP that might have been cleaved from the chimeric protein. The 153-kDa band detected with anti-Clag3.1 serum corresponds to the size of the endogenous Clag3.1. The rabbit anti-Clag3.1 serum identifies a single 153-kDa band in the wild type parasite extracts, which is consistent with the size of the endogenous Clag3.1; whereas the anti-GFP mAb does not recognize proteins in the wild type parasite extracts.

Following the expression of this chimeric protein during the erythrocytic cycle showed identical trafficking pattern to those of RhopH2-Myc-GFP and RhopH2-GFP, which ended with the translocation of this chimera to the apical end of the newly formed merozoites in the late schizont stage parasites (Fig. 7A, rows i–iv). The double immunofluorescence assay performed in the same way as above confirmed that this chimeric protein was specifically targeted to the rhoptries (Fig. 7B).

3.5. The N-terminal one third of Clag3.1 can not associate with the RhopH complex as a GFP chimeric protein

To determine if the conserved domain located in the N-terminal region of Clag3.1 contributes to the RhopH complex formation, we performed immunoprecipitation assays using protein extracts from transgenic parasites expressing the RhopH2-Myc-Clag3.1$_{(24-483)}$-GFP chimeric protein. The PfRhopH complex was immunoprecipitated with rabbit anti-RhopH2 serum and Western blot was performed with anti-RhopH2 mAb 4E10, mouse anti-Clag9 serum, and anti-GFP mAb. The chimeric protein was not detected following immunoprecipitation, whereas RhopH2 and Clag9 were successfully detected in the immunoprecipitated RhopH complex (Fig. 8). This indicates that the chimeric protein possessing the N-terminal 460 amino acids of Clag3.1 is incapable of associating with the RhopH complex as GFP-chimeric protein.

3.6. The C-terminus of Clag3.1 is not necessary for associating the RhopH complex

Aiming to generate positive control to investigate the Clag3.1 region possessing a RhopH complex-associating motif, we generated the transfection vector pH.RGDT-Clag3.1-Full which encodes the full length of Clag3.1 as a fusion protein with c-Myc at its N-terminus and GFP at its C-terminus. Transgenic parasites maintaining this construct as a stable episome did not show any green fluorescent signal when examined alive. Western blot analysis of transfected parasite extracts using mouse anti-GFP mAb did not show any signal. However, probing the same parasite extract with mouse anti-c-Myc mAb recognized one clear 120-kDa band (Fig. 9A). Probing non-transfected parasite extracts with anti-c-Myc did

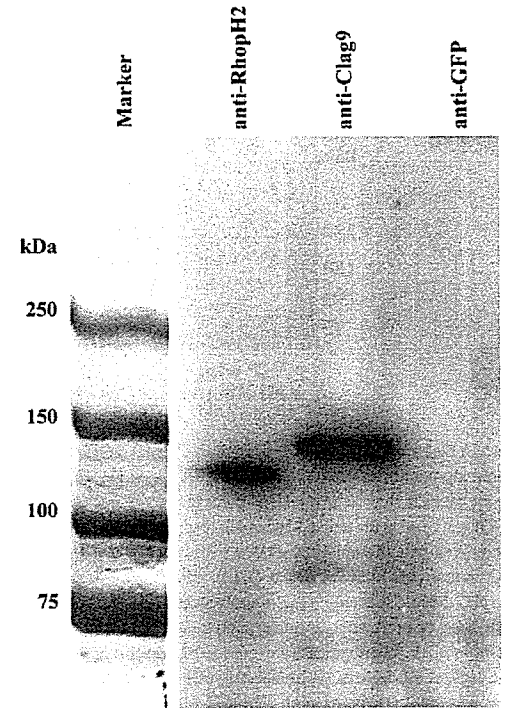

Fig. 8. Western blot analysis of the PfRhopH complex immunoprecipitated with rabbit anti-RhopH2 serum. Membranes were probed with mouse anti-RhopH2 (mAb 4E10), mouse anti-Clag9, or anti-GFP mAb. Both of RhopH2 and Clag9 were successfully detected, while the RhopH2-Myc-Clag3.1$_{(24\ 483)}$-GFP chimeric protein was not.

not show any signal (not shown). Thus, the 120-kDa band represents a truncated Clag3.1 that retains c-Myc at its N-terminus but lost GFP plus a 40-kDa C-terminal region of Clag3.1 (Fig. 2). Hence this chimeric protein was designated RhopH2-Myc-Clag3.1$_{115\ kDa}$. Nucleotide substitutions were evaluated by sequencing plasmids recovered from the transfected parasite line, however, no substitution resulting frameshift and/or stop codon were found. Thus, the inability to detect GFP plus the 40-kDa C-terminal region suggests that this small Clag3.1-GFP chimera has been degraded immediately after expression. Another possibility could be a translational arrest during the expression of this long chimeric protein, in this case around 184 kDa, from an episomal plasmid.

To investigate whether the RhopH2-c-Myc-Clag3.1$_{115\ kDa}$ can associate the RhopH complex, we immunoprecipitated RhopH complex with rabbit anti-RhopH2 serum and probed with anti-c-Myc mAb. The chimeric protein was successfully detected in the immunoprecipitated complex in addition to RhopH2 and Clag9, the positive controls (Fig. 9B). Reciprocally, we immunoprecipitated RhopH complex with anti-c-Myc mAb and probed with rabbit anti-RhopH2 serum, rabbit anti-Clag9 serum, anti-c-Myc mAb, and rabbit anti-Clag3.1 serum. RhopH2 was successfully co-precipitated with the chimeric protein, but Clag9 and the endogenous Clag3.1 were not co-precipitated. These data indicate that the C-terminus of Clag3.1 is not necessary for associating the RhopH complex. In

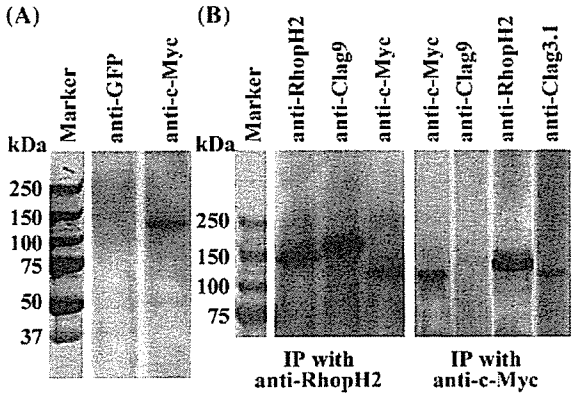

Fig. 9. Western blot analysis of the RhopH2-Myc-Clag3.$1_{115\ kDa}$ chimeric protein and the immunoprecipitated PfRhopH complex. (A) A single 120-kDa band was detected in the extracts from schizont stage parasites transfected with the construct pH.RGDT-Glag3.1Full with anti-c-Myc mAb, but not with anti-GFP mAb. (B) PfRhopH complex was immunoprecipitated with rabbit anti-RhopH2 serum and probed with mouse anti-RhopH2 (mAb 4E10), mouse anti-Clag9, or anti-c-Myc mAb. RhopH2-Myc-Clag3.$1_{115\ kDa}$ was successfully co-precipitated with RhopH2. In case of reciprocal immunoprecipitation of the PfRhopH complex with anti-c-Myc mAb, membranes were probed with rabbit anti-RhopH2 serum, rabbit anti-Clag9, anti-c-Myc mAb, or rabbit anti Clag3.1. In this case too, RhopH2 was successfully co-precipitated with RhopH2-Myc-Clag3.$1_{115\ kDa}$ but neither Clag9 nor the endogenous Clag3.1 was detected in this complex.

addition, the incorporation of RhopH2-c-Myc-Clag3.$1_{115\ kDa}$ into the RhopH complex prevented the incorporation of Clag9 and Clag3.1 into the same RhopH complex, supporting the previous proposal that each RhopH complex contains only one RhopH1/Clag family member [12].

4. Discussion

To study rhoptry protein expression and trafficking we have developed new transfection vectors for manipulating *Plasmodium* rhoptry proteins as GFP chimeras. Our results show that targeting proteins to the rhoptries follow the secretory pathway and only N-terminal 24 amino acids including a signal peptide sequence and correct expression timing are sufficient. Before being targeted to the rhoptries, proteins expressed from our constructs were seen accumulated in a cellular compartment that is likely the PV. We also showed that the C-terminus of Clag3.1 is not necessary for associating the RhopH complex.

The vector pRGDT-B12 developed in this study was designed to allow the production of tagged proteins with either or both c-Myc and GFP. The vector can be manipulated by the Gateway technology and allows easy cloning of genes of interest by single step ligation reactions that are faster and more efficient than the conventional ligation procedures. The resultant chimeric protein is expressed under the control of the *pfrhoph2* promoter. Due to the high AT content in *P. falciparum* genome, especially in the intergenic regions (86.4% AT content), the promoter sequences cloned from this pathogen are still very few and so far there is no report about cloning of any rhoptry gene promoter. Expression of the transgene under the *rhoph2* promoter was shown to be maximal in schizont stages. The precise timing of transgene expression has been shown to be critical for correct trafficking and subcellular localization of transgene products [32,33]; and thus these expression vectors will serve as valuable tools in studying the trafficking and expression of rhoptry and other proteins that are expressed in the late intra-erythrocytic parasite stages. The slightly earlier expression of the transgene could be due to a leaky expression from the *rhoph2* promoter in the episomal context, or due to the lack of additional upstream promoter elements needed for very tightly controlled timing of expression [32]. Notably, GFP fluorescence was detected only in schizont stages, and thus high levels of translated protein are relegated to mature intra-erythrocytic stages.

To explore the mechanism of protein targeting to rhoptries, we produced two GFP-expressing stable parasite lines and followed the trafficking pattern of GFP. Since, all proteins identified or predicted to be secreted from the apical organelles, rhoptries and micronemes, contain N-terminally located ER signal peptide sequence, we first showed by Western blot analysis that GFP fused to c-Myc and the signal peptide of RhopH2 appeared to be retained as an immature form, then later ER signal peptide was cleaved. This indicates that GFP fused with RhopH2 signal peptide is translocated to the ER post-translationally and this feature may reflect a specific nature of the RhopH2 signal sequence. According to Schatz and Dobberstein [34], the signal sequence mediates not only recognition of a protein by the membrane-linked transport system, but it can also have other functions such as determining whether transport into the ER occurs co- or post-translationally [35].

Our data conclusively show that RhopH2 signal peptide sequence plus only 5 amino acids downstream to the signal peptide cleavage site are able to target GFP to the rhoptries under the *rhoph2* promoter. Recently, Treeck et al. [36] showed that GFP fused with N-terminal 36 amino acids of microneme protein EBA-175 including predicted signal peptide sequence (21 aa), followed by EBA-175 transmembrane domain were not able to target to the apical organelle under *ama1* promoter, for which maximal expression can be seen at schizont stage, similar timing to the *rhoph2* promoter. This observation suggests that the timing of the expression is not the definitive factor of the rhoptry targeting. There are no reports of rhoptry targeting signal in *Plasmodium*, but at least 2 cases have been reported in the other apicomplexan parasite, *Toxoplasma gondii*. For example, TgROP1 can be targeted to the rhoptries with either the propeptide region (aa 1–85) including ER signal peptide sequence or a 372 amino acid central fragment [37]. Another case is TgROP4, for which the rhoptry targeting was originally proposed to be mediated by a C-terminal Tyr-based motif (YXXø) [38], but recent report showed that the N-terminal 163 amino acids, including ER signal peptide sequence, is sufficient for directing a GFP fusion protein to the rhoptries [39]. Together with these reports, our results suggest that N-terminal sequence around signal peptide have the capacity to target rhoptry proteins to their destination when expressed at schizont stage.

In *E. coli*, the signal sequence can act as a true targeting signal because it is specifically recognized by a cytosolic chaperone or targeting factor [34]. For example, the translocation of periplasmic alkaline phosphatase and maltose binding protein was suggested to depend on the chaperone DnaK

(*E. coli* homologue of Hsp70) [40] and the hydrophobic signal sequences of these proteins were found to constitute DnaK binding sites suggesting that the role of DnaK in translocation of these proteins relies on direct association with the signal sequence [41]. In yeast, a member of the Hsp70 family in the ER termed BiP is bound to a lumenally exposed DnaJ-like domain of Sec63p, a transmembrane subunit of the Sec63 complex [42–44]. This Hsp70 on the inner side of the ER membrane interacts with the translocating polypeptide chain and pulls it across the membrane [For details, see Refs. [34,45]]. In *P. falciparum*, mutating some amino acid residues predicted to be a part of the chaperone binding sites preceding the conserved host cell targeting motif (HCT or PEXEL motif) resulted in a significant retention of a portion of the chimeric STEVOR protein within the parasite's ER [46]. Similarly, the putative Hsp70 (DnaK) binding sites present in the transit peptide proved to be important for correct targeting of proteins to the apicoplast [31]. These results imply an auxiliary or alternative role for parasite chaperones in protein targeting. The study of Sargeant et al. [47] to predict the exported proteins in the genus *Plasmodium*, showed the presence of chaperone binding sites in many of the well known and predicted exported proteins families together with a family of putative DnaJ domain-containing co-chaperones, implying a role for these co-chaperones in the translocation process and correct conformation of some of these proteins (e.g. PfEMP1 complex).

Based on the above-mentioned reports, we suggest that the chimeric proteins in this study were recognized by a chaperone, for example Hsp70 family or its homologues, in the ER matrix through interaction with the first 24 amino acid sequence of the RhopH2 including signal peptide. A simultaneous binding to the mature proteins by a specific co-chaperone or co-factor would then mark these proteins for binding with a rhoptry-targeted molecule. In fact, Topolska et al. [5] has identified a rhoptry protein RAMA (rhoptry-associated membrane antigen) that is synthesized several hours before rhoptry formation (the earliest expressed rhoptry protein) and transiently localizes within the ER and Golgi within lipid-rich microdomains and some other rhoptry proteins such as RhopH3 and RAP1 were found in close apposition with RAMA.

The accumulation of both of the chimeric proteins in the PV of the schizont stages before the appearance of any rhoptry vesicles shows a typical "necklace-of-beads" pattern described for the PV localization of GFP chimeras of the exported proteins KAHRP, Exp1, and RESA [19,21,32]. Such pattern was suggested to represent either vesicular compartments involved in the transport of the fluorescent protein to the PV, or subcompartments within the PV [19]. Recent reports suggested that rhoptry proteins might have a function in the PV before rhoptry formation. For example, RhopH3 was transiently localized to the PV before rhoptry formation [48] and the proteome analysis identified newly synthesized rhoptry proteins, RhopH2 and RAP3, in the membranous network fraction [17]. Based on these data, the RhopH complex was proposed to be a possible candidate translocon mediating export of proteins through the PV [16]. Whether these accumulations are just default depot as reported [18,19,21,32] due to an earlier timing of expression of our chimeric proteins before rhoptry formation or for a functional role in the PV is yet to be determined.

In this report, we evaluated, for the first time, the role of a recognizable conserved domain in the RhopH complex formation. This domain is located at the N-terminus of RhopH1 and has apparent homology with PF14_0495. PF14_0495 is encoded in single exon and an orthologous protein TgRON2 was recently identified in *T. gondii* and proposed to make a complex including TgAMA1 [49,50]. The results presented here show that RhopH2-Myc-Clag3.1$_{(24–483)}$-GFP chimeric protein can not associate the RhopH complex and the C-terminus of Clag3.1 is not necessary for associating the RhopH complex. We should note that there is a possibility that a potential RhopH complex association of the Clag3.1$_{(24–483)}$ part might be interfered by fusing with GFP. The C-terminal part of the chimeric Clag3.1 is estimated to be chopped off after the eleventh Cys residue in Clag3.1 which represents the tenth and the last Cys residue conserved among all members of RhopH1/Clag family. With respect to amino acid sequence conservation among parasite lines, members of the RhopH1/Clag family show most of the variation in the C-terminus [unpublished data]. Thus, the region where the RhopH complex-associating motif locates appears to be conserved among parasite lines.

In summary, we have expressed GFP and Clag3.1-GFP as fusion proteins with RhopH2 signal peptide under *rhoph2* promoter to show that targeting of the rhoptry proteins is mediated by unknown mechanism probably involving the interaction of some chaperones with RhopH2 signal peptide early in the ER and the interaction of rhoptry-targeted molecules. Incorporation into the RhopH complex can not be accomplished by the interaction of the N-terminal one third of Clag3.1 as a GFP chimera but a truncated Clag3.1 lacking the C-terminal region successfully associated the RhopH complex suggesting that cooperation of the middle region is probably required and that the C-terminus of Clag3.1 is not necessary for the RhopH complex formation.

Acknowledgements

We thank T. Templeton for the critical reading and helpful comments. We are grateful to A. Cowman for providing pHH1, D. Jacobus for WR99210, A. Holder and I. Ling for rabbit anti-PfRhopH2 serum and mAb 4E10, C. Long for rabbit anti-AMA1 serum and D. Mattei for rabbit anti-Clag9 serum. pHRPGFPm2 (MRA-69) was provided by K. Haldar through MR4. A. G. was supported through the scholarship Kh149 from the Ministry of Higher Education and Scientific Research, Egyptian government. This work was supported in part by Grants-in-Aid for Scientific Research 16390126 (to M. T.) and 17590372 (to O. K.) from the Ministry of Education, Culture, Sports, Science and Technology, Japan.

References

[1] Bannister LH, Mitchell GH, Butcher GA, Dennis ED. Lamellar membranes associated with rhoptries in erythrocytic merozoites of *Plasmodium knowlesi*: a clue to the mechanism of invasion. Parasitology 1986;92:291–303.

[2] Sam-Yellowe TY, Shio H, Perkins ME. Secretion of *Plasmodium falciparum* rhoptry protein into the plasma membrane of host erythrocytes. J Cell Biol 1988;106:1507–13.

[3] Bannister LH, Hopkins JM, Fowler RE, Krishna S, Mitchell GH. Ultrastructure of rhoptry development in *Plasmodium falciparum* erythrocytic schizonts. Parasitology 2000;121:273–87.
[4] Jaikaria NS, Rozario C, Ridley RG, Perkins ME. Biogenesis of rhoptry organelles in *Plasmodium falciparum*. Mol Biochem Parasitol 1993;57:269–79.
[5] Topolska AE, Lidgett A, Truman D, Fujioka H, Coppel RL. Characterization of a membrane-associated rhoptry protein of *Plasmodium falciparum*. J Biol Chem 2004;279:4648–56.
[6] Campbell GH, Miller LH, Hudson D, Franco EL, Andrysiak PM. Monoclonal antibody characterization of *Plasmodium falciparum* antigens. Am J Trop Med Hyg 1984;33:1051–4.
[7] Holder AA, Freeman RR, Uni S, Aikawa M. Isolation of a *Plasmodium falciparum* rhoptry protein. Mol Biochem Parasitol 1985;14:293–303.
[8] Cooper JA, Ingram LT, Bushell GR, Fardoulys CA, Stenzel D, Schofield L, et al. The 140/130/105 kilodalton protein complex in the rhoptries of *Plasmodium falciparum* consists of discrete polypeptides. Mol Biochem Parasitol 1988;29:251–60.
[9] Hienne R, Ricard G, Fusaï T, Fujioka H, Pradines B, Aikawa M, et al. *Plasmodium yoelii*: identification of rhoptry proteins using monoclonal antibodies. Exp Parasitol 1998;90:230–5.
[10] Kaneko O, Tsuboi T, Ling IT, Howell S, Shirano M, Tachibana M, et al. The high molecular mass rhoptry protein, RhopH1, is coded by members of the *clag* multigene family in *Plasmodium falciparum* and *Plasmodium yoelii*. Mol Biochem Parasitol 2001;118:223–31.
[11] Ling IT, Florens L, Dluzewski AR, Kaneko O, Grainger M, Yim Lim BYS, et al. The *Plasmodium falciparum clag9* gene encodes a rhoptry protein that is transferred to the host erythrocyte upon invasion. Mol Microbiol 2004;52:107–18.
[12] Kaneko O, Yim Lim BYS, Iriko H, Ling IT, Otsuki H, Grainger M, et al. Apical expression of three RhopH1/Clag proteins as components of the *Plasmodium falciparum* RhopH complex. Mol Biochem Parasitol 2005;143:20–8.
[13] Ling IT, Kaneko O, Narum DL, Tsuboi T, Howell S, Taylor HM, et al. Characterisation of the *rhoph2* gene of *Plasmodium falciparum* and *Plasmodium yoelii*. Mol Biochem Parasitol 2003;127:47–57.
[14] Sam-Yellowe TY. Molecular factors responsible for host cell recognition and invasion in *Plasmodium falciparum*. J Protozool 1992;39:181–9.
[15] Rungruang T, Kaneko O, Murakami Y, Tsuboi T, Hamamoto H, Akimitsu N, et al. Erythrocyte surface glycosylphosphatidyl inositol anchored receptor for the malaria parasite. Mol Biochem Parasitol 2005;140:13–21.
[16] Lanzer M, Wickert H, Krohne G, Vincensini L, Braun-Breton C. Maurer's clefts: a novel multi-functional organelle in the cytoplasm of *Plasmodium falciparum*-infected erythrocytes. Int J Parasitol 2006;36:23–36.
[17] Vincensini L, Richert S, Blisnick T, Van Dorsselaer A, Leize-Wagner E, Rabilloud T, et al. Proteomic analysis identifies novel proteins of the Maurer's clefts, a secretory compartment delivering *Plasmodium falciparum* proteins to the surface of its host cell. Mol Cell Proteomics 2005;4:582–93.
[18] Waller RF, Reed MB, Cowman AF, McFadden GI. Protein trafficking to the plastid of *Plasmodium falciparum* is via the secretory pathway. EMBO J 2000;19:1794–802.
[19] Wickham ME, Rug M, Ralph SA, Klonis N, McFadden GI, Tilley L, et al. Trafficking and assembly of the cytoadherence complex in *Plasmodium falciparum*-infected human erythrocytes. EMBO J 2001;20:5636–49.
[20] Cheresh P, Harrison T, Fujioka H, Haldar K. Targeting the malarial plastid via the parasitophorous vacuole. J Biol Chem 2002;277:16265–77.
[21] Adisa A, Rug M, Klonis N, Foley M, Cowman AF, Tilley L. The signal sequence of exported protein-1 directs the green fluorescent protein to the parasitophorous vacuole of transfected malaria parasites. J Biol Chem 2003;278:6532–42.
[22] Marti M, Good RT, Rug M, Knuepfer E, Cowman AF. Targeting malaria virulence and remodeling proteins to the host erythrocyte. Science 2004;306:1930–3.
[23] Hiller NL, Bhattacharjee S, van Ooij C, Liolios K, Harrison T, Lopez-Estrano C, et al. A host-targeting signal in virulence proteins reveals a secretome in malarial infection. Science 2004;306:1934–7.
[24] Reed MB, Saliba KJ, Caruana SR, Kirk K, Cowman AF. Pgh1 modulates sensitivity and resistance to multiple antimalarials in *Plasmodium falciparum*. Nature 2000;403:906–9.
[25] VanWye JD, Haldar K. Expression of green fluorescent protein in *Plasmodium falciparum*. Mol Biochem Parasitol 1997;87:225–9.
[26] Trager W, Jensen JB. Human malaria parasites in continuous culture. Science 1976;193:673–5.
[27] Deitsch K, Driskill C, Wellems T. Transformation of malaria parasites by the spontaneous uptake and expression of DNA from human erythrocytes. Nucleic Acids Res 2001;29:850–3.
[28] Staalsoe T, Giha HA, Dodoo D, Theander TG, Hviid L. Detection of antibodies to variant antigens on *Plasmodium falciparum*-infected erythrocytes by flow cytometry. Cytometry 1999;35:329–36.
[29] Taylor HM, Grainger M, Holder AA. Variation in the expression of a *Plasmodium falciparum* protein family implicated in erythrocyte invasion. Infect Immun 2002;70:5779–89.
[30] Kaneko O, Fidock DA, Schwartz OM, Miller LH. Disruption of the C-terminal region of EBA-175 in the Dd2/Nm clone of *Plasmodium falciparum* does not affect erythrocyte invasion. Mol Biochem Parasitol 2000;110:135–46.
[31] Foth BJ, Ralph SA, Tonkin CJ, Struck NS, Fraunholz M, Roos DS, et al. Dissecting apicoplast targeting in the malaria parasite *Plasmodium falciparum*. Science 2003;299:705–8.
[32] Rug M, Wickham ME, Foley M, Cowman AF, Tilley L. Correct promoter control is needed for trafficking of the ring-infected erythrocyte surface antigen to the host cytosol in transfected malaria parasites. Infect Immun 2004;72:6095–105.
[33] Kocken CH, van der Wel AM, Dubbeld MA, Narum DL, van de Rijke FM, van Gemert GJ, et al. Precise timing of expression of a *Plasmodium falciparum*-derived transgene in *Plasmodium berghei* is a critical determinant of subsequent subcellular localization. J Biol Chem 1998;273:15119–24.
[34] Schatz G, Dobberstein B. Common principles of protein translocation across membranes. Science 1996;271:1519–26.
[35] Walter P, Johnson AE. Signal sequence recognition and protein targeting to the endoplasmic reticulum membrane. Annu Rev Cell Biol 1994;10:87–119.
[36] Treeck M, Struck NS, Haase S, Langer C, Herrmann S, Healer J, et al. A conserved region in the EBL proteins is implicated in microneme targeting of the malaria parasite *Plasmodium falciparum*. J Biol Chem 2006;281:31995–2003.
[37] Striepen B, Soldati D, Garcia-Reguet N, Dubremetz J, Roos D. Targeting of soluble proteins to the rhoptries and micronemes in *Toxoplasma gondii*. Mol Biochem Parasitol 2001;113:45–53.
[38] Hoppe HC, Ngo HM, Yang M, Joiner KA. Targeting to rhoptry organelles of *Toxoplasma gondii* involves evolutionarily conserved mechanisms. Nat Cell Biol 2000;2:449–56.
[39] Bradley PJ, Li N, Boothroyd JC. A GFP-based motif-trap reveals a novel mechanism of targeting for the *Toxoplasma* ROP4 protein. Mol Biochem Parasitol 2004;137:111–20.
[40] Wild J, Altman E, Yura T, Gross CA. DnaK and DnaJ heat shock proteins participate in protein export in *Escherichia coli*. Genes Dev 1992;6:1165–72.
[41] Rudiger S, Germeroth L, Schneider-Mergener J, Bukau B. Substrate specificity of the DnaK chaperone determined by screening cellulose-bound peptide libraries. EMBO J 1997;16:1501–7.
[42] Sanders SJ, Whiffield KM, Vogel JP, Rose MD, Schekman RW. Sec61p and BiP directly facilitate polypeptide translocation into the ER. Cell 1992;69:353–65.
[43] Brodsky JL, Schekman R. A Sec63p–BiP complex from yeast is required for protein translocation in a reconstituted proteoliposome. J Cell Biol 1993;123:1355–63.
[44] Panzner S, Dreier L, Hartmann E, Kostka S, Rapoport TA. Posttranslational protein transport in yeast reconstituted with a purified complex of Sec proteins and Kar2p. Cell 1995;81:561–70.
[45] Neupert W, Brunner M. The protein import motor of mitochondria. Nat Rev Mol Cell Biol 2002;3:555–65.
[46] Przyborski JM, Miller SK, Pfahler JM, Henrich PP, Rohrbach P, Crabb BS, et al. Trafficking of STEVOR to the Maurer's clefts in *Plasmodium falciparum*-infected erythrocytes. EMBO J 2005;24:2306–17.
[47] Sargeant TJ, Marti M, Caler E, Carlton JM, Simpson K, Speed TP, et al. Lineage-specific expansion of proteins exported to erythrocytes in malaria parasites. Genome Biol 2006;7:R12.

[48] Sam-Yellowe TY, Fujioka H, Aikawa M, Hall T, Drazba JA. A *Plasmodium falciparum* protein located in Maurer's clefts underneath knobs and protein localization in association with Rhop-3 and SERA in the intracellular network of infected erythrocytes. Parasitol Res 2001;87:173–85.
[49] Bradley PJ, Ward C, Cheng SJ, Alexander DL, Coller S, Coombs GH, et al. Proteomic analysis of rhoptry organelles reveals many novel constituents for host–parasite interactions in *Toxoplasma gondii*. J Biol Chem 2005;280:34245–58.
[50] Alexander DL, Mital J, Ward GE, Bradley P, Boothroyd JC. Identification of the moving junction complex of *Toxoplasma gondii*: a collaboration between distinct secretory organelles. PLoS Pathog 2005;1:137–49.

International Immunology, Vol. 19, No. 1, pp. 67–79
doi:10.1093/intimm/dxl123

Pathological role of Toll-like receptor signaling in cerebral malaria

Cevayir Coban[1,2]*, Ken J. Ishii[1,3]*, Satoshi Uematsu[1], Nobuko Arisue[4], Shintaro Sato[1,3], Masahiro Yamamoto[1], Taro Kawai[1,3], Osamu Takeuchi[1,3], Hajime Hisaeda[5], Toshihiro Horii[4] and Shizuo Akira[1,2,3]

[1]Department of Host Defense, Research Institute for Microbial Diseases, [2]21st Century Center of Excellence, Combined Program on Microbiology and Immunology, [3]Exploratory Research for Advanced Technology, Japan Science and Technology Agency and [4]Department of Molecular Protozoology, Research Institute for Microbial Diseases, Osaka University, Suita, Osaka 565-0871, Japan
[5]Department of Parasitology, Graduate School of Medical Sciences, Kyushu University, Fukuoka 812-8582, Japan

Keywords: cell trafficking, hemozoin, innate immunity, MyD88, *Plasmodium*

Abstract

Toll-like receptors (TLRs) recognize malaria parasites or their metabolites; however, their physiological roles in malaria infection *in vivo* are not fully understood. Here, we show that myeloid differentiation primary response gene 88 (MyD88)-dependent TLR signaling mediates brain pathogenesis of severe malaria infection, namely cerebral malaria (CM). A significant number of MyD88-, but not TIR domain containing adaptor-inducing IFN-beta (TRIF)-deficient or wild-type (WT) mice survived CM caused by *Plasmodium berghei* ANKA (PbA) infection. Although systemic parasitemia was comparable, sequestration of parasite and hemozoin load in the brain blood vessels was significantly lower in MyD88-deficient mice compared with those in TRIF-deficient or WT mice. Moreover, brain-specific pathological changes were associated with MyD88-dependent infiltration of $CD8^+$, $CCR5^+$ T cells and $CD11c^+$ dendritic cells, including $CD11c^+$, $NK1.1^+$ and $B220^+$ cells, and up-regulation of genes such as *Granzyme B*, *Lipocalin 2*, *Ccl3* and *Ccr5*. Further studies using mice lacking various TLRs suggest that TLR2 and TLR9, but not TLR4, 5 and 7, were involved in CM. These results strongly suggest that TLR2- and/or TLR9-mediated, MyD88-dependent brain pathogenesis may play a critical role in CM, the lethal complication during PbA infection.

Introduction

Cerebral malaria (CM) is the lethal complication of malaria caused by *Plasmodium falciparum* in humans. Besides the high mortality rates, persistent neurocognitive deficits after recovery have become an increasing concern in past decades (1–3). While precise molecular and cellular mechanisms underlying the pathogenesis of CM are not yet fully elucidated, *Plasmodium berghei* ANKA (PbA) infection in mice provides valuable information as an experimental model of CM (4–6). After infection with PbA, susceptible mice (e.g. C57Bl/6) develop symptoms within a week, such as ataxia, hemi- or paraplegia, seizures and coma, and die within the following 24 h. Profound intravascular changes occur in cerebral vessels, such as endothelial cell damage and sequestration of infected erythrocytes, as well as host immune cells (i.e. platelets and leukocytes).

In recent decades, host immune responses to parasites have been implicated in playing an important role in CM pathogenesis. For example: (i) systemic pro-inflammatory cytokines such as IL-12, IFNγ and tumor necrosis factor (TNF) α, but not IL-1 or IL-18 (7–9); and (ii) specific cell types, such as CD1d-restricted NK T cells and $CD8^+$ T cells (10, 11), have been reported as critical mediators in CM development. Immune cell trafficking through CCR5 but not CCR2 has been found to be critical for leukocyte accumulation in the brain of CM-susceptible mice (12). However, the precise mechanism by which innate immune receptors or their signaling triggers such brain as well as systemic inflammation and immune cell trafficking is not known.

Toll-like receptors (TLRs) have been identified as key host molecules in innate immune recognition of and response to

*These authors contributed equally to this study.

Correspondence to: S. Akira; E-mail: sakira@biken.osaka-u.ac.jp

Transmitting editor: K. Inaba

Received 23 August 2006, *accepted* 24 October 2006

Advance Access publication 29 November 2006

microbial products including lipids, proteins and nucleic acids (13). Recent evidence suggests that TLRs are involved in the innate immune responses to *Plasmodium* species (14). Adachi *et al.* (15) for the first time has analyzed the involvement of TLRs *in vivo* using a mouse malaria infection model where myeloid differentiation primary response gene 88 (MyD88), an essential adaptor molecule for most TLRs, is critical for IL-12 induction by *P. berghei* NK65 parasites, causing liver injury. Recently, glycosyl-phosphatidylinositol (GPI) and hemozoin (a parasite heme metabolite) derived from *P. falciparum* have been identified as the ligands for TLR2 and TLR9, respectively (16, 17), whereas other heat-labile molecules derived from the malaria parasite are still to be clarified for TLR9-mediated recognition (18).

Based on the above findings, we investigated the role of TLRs and their signaling molecules in the pathogenesis of CM. We used an *in vivo* experimental model for CM in which various mutant mice lacking TLRs and their adaptor molecules, such as MyD88 and TIR domain containing adaptor-inducing IFN-beta (TRIF), were infected with PbA. Monitoring survival, CM symptoms, parasitemia, hemoglobin level, pathological changes in the brain and host immune responses after infection revealed that TLR2-, TLR9- and MyD88-dependent signaling, but not TLR4-, TLR5-, TLR7- or TRIF-dependent signaling, facilitated CM pathogenesis and its resultant mortality. Analysis of systemic, as well as local inflammatory responses, suggest that the TLR–MyD88-dependent CM pathogenesis was associated with not only systemic inflammatory responses but also with brain sequestration of parasite, as well as hemozoin, and infiltration of particular lymphocytes, such as $CCR5^+$, $CD8^+$ T cells and $CD11c^+$ dendritic cells (DCs) including $NK1.1^+$, $B220^+$ and $CD11c^+$ cells, expressing both DC and NK cell marker.

Methods

Animals

Mice deficient for MyD88, TRIF, TLR2, TLR4, TLR5, TLR7 or TLR9 were generated as described previously (19–25). Except $TRIF^{-/-}$ mice and their littermate controls which are on a 129/Ola × C57Bl/6 (B6.129) background, all mice used here were backcrossed to C57Bl/6 (B6) background at least for eight generations. Age (6–10 weeks old)- and sex-matched groups of wild-type (WT) (either purchased from CLEA, Japan, or wild-type littermates) and knockout mice were used in the experiments. Animal experiments for infection were approved by the institutional protocol of the Research Institute for Microbial Diseases, Osaka University.

PbA infection and CM assessment

First, donor mice (either B6 or B6.129) were infected with the frozen stock of PbA-infected RBCs (iRBCs), and 6–7 days later, when the parasitemia showed mostly ring stages, and the mice suffered from CM symptoms, blood was drawn and used for infection studies. We chose this method to infect each mouse with similar blood-stage parasites. Then, WT or various mutant mice were infected with 10^6 iRBCs intra-peritoneally in 200 µl PBS. Parasitemia was assessed every 2 days by microscopy of Giemsa-stained thin blood smears. Survival and signs of disease were monitored daily. Animals that showed neurological signs, such as convulsions, ataxia and paralysis, and died between 6 and 12 days after infection were considered as having CM. Brains were removed and used for histological analysis and reverse transcription (RT)–PCR. Serum was taken for cytokine ELISA and kept at –80°C until use. Blood hemoglobin levels were analyzed by using Drabkin's solution, as described elsewhere (12).

Cell culture, PbA crude extract and hemozoin

The murine microglial cell line BV-2 was cultured in 10% fetal bovine serum (FBS)-containing DMEM medium as described before (26). One million cells ml^{-1} were seeded on to a six-well culture plate and stimulated for 24 h as indicated. Then, cells were collected, and total RNA was extracted using TRIzol reagent. RT-PCR was performed as mentioned below. PbA crude extract was prepared from the blood of infected mice, as described elsewhere (27). Hemozoin was prepared from *Mycoplasma*-free *P. falciparum* cultures as described before (17). CpG ODN 1555 was used as a control stimulant (26).

Histology

Six days after PbA infection, brains were perfused with PBS and carefully removed and fixed in formaldehyde solution (4% v/v). Tissue sections were prepared and stained with hematoxylin and eosin (HE) as described elsewhere (10). The sections were also stained by Prussian blue in order to visualize and count the hemozoin clusters. After staining with potassium ferrocyanide, counterstaining with nuclear fast red solution allowed us to visualize dark brown hemozoin clusters that were easily counted by light microscopy (Fig. 2B).

Flow cytometry of brain-infiltrating lymphocytes

On day 6 after PbA infection, lymphocytes from brain were isolated as previously described (12). Briefly, after perfusion with PBS to remove the circulating blood cells, brains were crushed and washed in RPMI 1640 medium supplemented with 10% FBS and penicillin–streptomycin. Brain tissue extracts were then pelleted by centrifugation at 400 × *g* for 5 min, and were further purified on a 30% Percoll gradient (Amersham) (400 × *g* for 30 min). Cells were counted, fixed and stained with FITC-, PE-, CyChrome- or allophycocyanin (APC)-labeled antibody in the presence of anti-CD16 antibody for 30 min at room temperature, as previously described (17). Stained cells were washed, re-suspended in PBS/0.1% BSA/0.1% NaN_3 and analyzed by FACSCalibur, followed by analysis using CellQuest software (Becton Dickinson). All antibodies used were purchased from Becton Dickinson. T cell staining was performed using CD8–APC (or –FITC), Thy1.2–PE, TCRβ–CyChrome, CD4–APC (or –FITC) and CCR5–PE. NK cells, B cells and DCs were stained with NK1.1–PE, CD45R (B220)–CyChrome and CD11c–APC (28, 29).

DNA microarray analysis

On day 6 of infection with PbA, half of the brain tissues were removed and kept at –80°C. Total RNA was extracted from individual brains with TRIzol and further purified by RNeasy

kit (Qiagen, Hilden, Germany), and cDNA was synthesized from total RNA with the SuperScript Choice System (Invitrogen, Carlsbad, CA, USA). These cDNAs were used to prepare biotin-labeled cRNA according to the manufacturer's protocol (Enzo Diagnostics, Farmingdale, NY, USA). Purification of cRNA and hybridization and scanning of the microarray were done according to the manufacturer's instructions (Affymetrix, MG U74A version 2). Data analysis was carried out by using a Suite software version 5.0 (Affymetrix) and GeneSpring software version 6.0 (Silicongenetics, Redwood, CA, USA) (30). To confirm the gene changes, the experiment was performed twice by using two mice per group.

RT-PCR

RT-PCR was carried out as described elsewhere (30). Briefly, brain tissues were homogenized and total RNA was extracted with TRIzol reagent (Invitrogen) according to the manufacturer's protocol. Then, 1 μg total RNA was reverse transcribed with SuperScript II (Invitrogen). PCR amplification was performed using recombinant *Taq* DNA polymerase (Takara Shuzo). PCR conditions were 30 s denaturation at 94°C, 30 s annealing at 60°C and 1 min elongation at 72°C for 30 cycles. Specific primers used were as follows: *Granzyme B*, sense 5′-TCGACCCTACATGGCCTTAC-3′ and anti-sense 5′-TGGG GAATGCATTTTACCAT-3′; Lipocalin 2, sense 5′-CCAGTTCGC CATGGTATTTT-3′ and anti-sense 5′-CACACTCACCACCCATT CAG-3′; MIP-1α, sense 5′-ATGAAGGTCTCCACCACTGCCC-AAGC-3′ and anti-sense 5′-TTAGTCAGGAAAATGACACCTG GCTGGG-3′; IL-6, sense 5′-GACAAAGCCAGAGTCCTTCAG AGAG-3′ and anti-sense 5′-CTAGGTTTGCCGAGTAGATCC TC-3′ and β-actin, sense 5′-GACATGGAGAAGATCTGGCAC CACA-3′ and anti-sense 5′-ATCTCCTGCTCGAAGTCTAGA-CAA-3′. Density of the PCR products in ethidium bromide-stained gel was measured by NIH image software (http://rsb.info.nih.gov/nih-image/download.html). Quantities of each transcript were compared with the β-actin reference.

ELISA

Mouse IFNγ, TNFα and IL-12p40 in the serum were measured by ELISA (DuoSet ELISA Kit, R&D Systems, Minneapolis, MN, USA) according to the manufacturer's instructions.

Statistical analysis

Differences between groups were analyzed for statistical significance by using SigmaStat 3.0 software with either Student's *t*-test or Mann–Whitney *U*-test. For survival curves, Kaplan–Meier plots and log rank tests were performed. $P < 0.05$ was considered statistically significant.

Results

Critical role of MyD88 in CM and its resultant lethality, but not in systemic parasitemia

MyD88 is an essential adaptor molecule for most TLR signaling, whereas TRIF is an indispensable adaptor for TLR3 and TLR4 (31). To examine the possible role of innate immune responses through TLRs in CM pathogenesis, we first infected intra-peritoneally MyD88- or TRIF-deficient mice with a C57Bl/6 (B6) or 129/Ola × C57Bl/6 (B6.129) background, then monitored their survival, parasitemia, percentage hemoglobin in the blood. B6.129 mice were susceptible to CM with 10^6 PbA and frequency of characteristic CM symptoms were consistent with a previous report (12). After infection, WT mice showed CM symptoms within 6–12 days and died within the following 24 h; however, a significant number of MyD88-deficient mice survived CM and eventually died of extremely high parasitemia, reaching >85% (Fig. 1A, $P = 0.003$ by log rank survival test). In sharp contrast, infected TRIF-deficient mice died even before the WT controls, during which all of the TRIF-deficient mice suffered from CM (Fig. 1B, $P = 0.325$ by log rank survival test). Overall survival from CM was significantly higher in MyD88-deficient mice than that in WT or TRIF-deficient mice [Fig. 1C and D, 10% of WT ($n = 50$) versus 46.15% of MyD88$^{-/-}$ ($n = 39$) mice escaped from CM; 9.1% of WT ($n = 16$) versus none of the TRIF$^{-/-}$ ($n = 16$) mice escaped from CM].

Systemic parasitemia and hemoglobin levels were comparable between WT and MyD88- and TRIF-deficient mice during the first week of PbA infection (Fig. 1A and B and data not shown), similar to a previous study on infection with *P. berghei* NK65 which did not cause CM (15). These data suggest that MyD88, but not TRIF, is involved in CM symptoms and subsequent death, whereas neither MyD88 nor TRIF is involved in controlling parasitemia or the resultant anemia.

MyD88-dependent parasite sequestration and hemozoin load in the brain

We investigated the mechanisms involved in the pathogenesis of MyD88-dependent CM. Since brain-specific immunopathological changes have been shown to play a critical role in CM development (4, 5, 32), we examined the effects of MyD88 and TRIF on immunopathological changes in the brains of mice 6 days after infection, at which most WT mice begin to develop characteristic symptoms of CM. Histological examination of brain sections revealed that WT mice from a B6 or B6.129 background, as well as TRIF-deficient mice, showed typical vascular occlusion with parasitized erythrocytes as well as leukocytes and microvascular destruction including endothelial cell detachment (Fig. 2A, b and c). However, these characteristic pathological changes were absent in MyD88- but not in TRIF-deficient mice, suggesting that a MyD88-dependent immune response may play a role in the brain pathogenesis of CM (Fig. 2A, d and e, respectively).

We have previously demonstrated that hemozoin, a malaria metabolite during the red blood cell stage, activates the innate immune system via TLR9 and MyD88 (17). To investigate whether hemozoin is involved in the pathogenesis of CM, we attempted to visualize hemozoin clusters in HE-stained brain sections. However, we found that when the sections were stained with Prussian blue, visualization was easier due to faint red staining of the background (Fig. 2B). We counted hemozoin clusters in 25 microvessels per group ($n = 3$ or 4) by light microscopy, and found that hemozoin accumulation was significantly reduced in MyD88-deficient brains compared with that in WT brains at day 6 (Fig. 2C, $P < 0.001$ by Mann–Whitney *U*-test), in spite of comparable systemic parasitemia levels (Fig. 1A).

In addition, we noticed that there was hemozoin residue in the tissues, outside the blood vessels (data not shown). It is

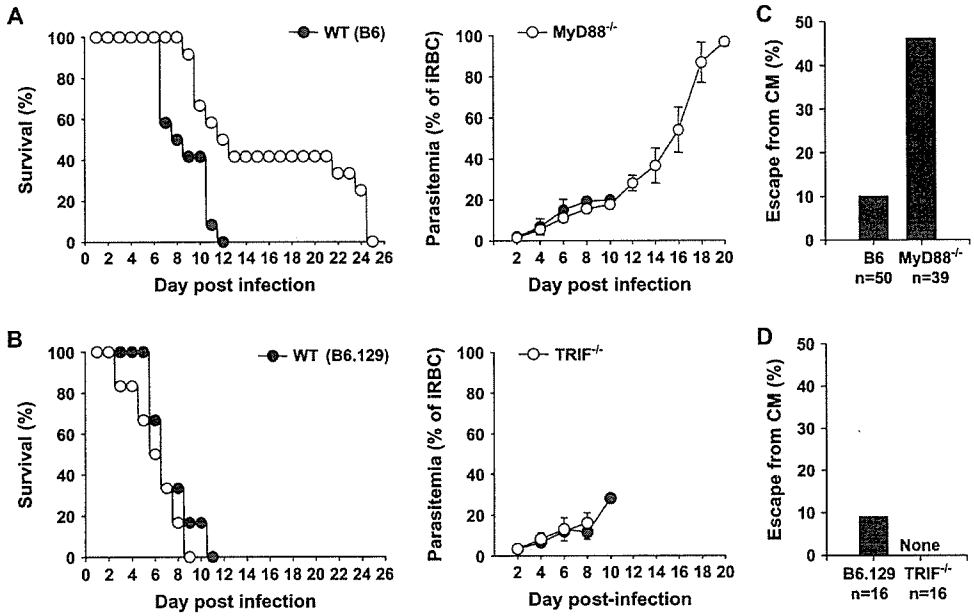

Fig. 1. MyD88- but not TRIF-deficient mice have increased resistance to CM. MyD88$^{-/-}$ and TRIF$^{-/-}$ mice and their WT controls were infected intra-peritoneally with 10^6 iRBCs of PbA strain. The percentage survival and parasitemia of (A) WT (B6, closed circles) and MyD88-deficient (MyD88$^{-/-}$, open circles) mice ($n = 12$ for each group) and (B) WT (B6.129, closed circles) and TRIF-deficient (TRIF$^{-/-}$, open circles) mice ($n = 6$ for each group, littermates) after infection. Survival was monitored daily. Parasitemia was assessed by Giemsa-stained blood smears every other day (mean parasitemia ± SE). Data shown here are representative of three (B) to six (A) different experiments ($P = 0.003$ for the percentage survival curve of WT versus MyD88$^{-/-}$ mice; $P = 0.327$ for those of WT versus TRIF$^{-/-}$ mice by log rank test). (C) Total escape from CM in MyD88$^{-/-}$ mice until day 12 after infection. Ten percent of WT (B6) mice ($n = 50$) escaped from CM versus 46.15% of MyD88$^{-/-}$ mice ($n = 39$). (D) Total escape from CM in TRIF$^{-/-}$ mice until day 12 after infection. In all, 9.1% of WT (B6.129) mice ($n = 16$) escaped from CM versus 0% of TRIF$^{-/-}$ mice ($n = 16$). 'None' implies that no TRIF$^{-/-}$ mice could survive.

possible that destruction of the blood–brain barrier might allow parasites or hemozoin itself to enter the brain tissue to activate residual microglia cells. Indeed, microglial cell activation during CM has previously been implicated (33), which prompted us to evaluate whether microglia cells, macrophage-like cells in the brain, can be directly activated by hemozoin or crude extract of iRBCs. We stimulated BV-2 cells (26) (a murine microglia cell line expressing TLR9 mRNA (34)) with PbA crude extract and hemozoin for 24 h (Supplementary Figure 1A and B, available at *International Immunology* Online). RT–PCR analysis showed activation by hemozoin or PbA crude extract in BV-2 cells to up-regulate mRNA expression of acute inflammatory response genes such as *Lipocalin 2*, *MIP-1α* and *IL-6*. We used CpG ODN 1555 as a control (26). Taken together, these data suggest that microglial cell line can respond to hemozoin and PbA crude extract.

Role of MyD88 and TRIF in the immunopathological changes in the brain during PbA infection

In order to comprehensively analyze and identify the genes involved in MyD88-dependent, brain-specific molecular events during CM, we obtained brains from WT mice or MyD88- or TRIF-deficient mice at day 6 after PbA infection, and examined their mRNA expression profiles by DNA microarray analysis. We compared 'fold increases' of mRNA expression in PbA-infected brain tissue over those in uninfected tissue, which were then compared with those of WT mice (B6 or B6.129) and MyD88- and TRIF-deficient mice. A cut-off value was determined as a 5-fold change in infected brains over that of uninfected WT mice. Genes that showed a <2-fold change between WT and mutant mice were determined as 'independent', whereas those with a >2-fold change were determined as 'dependent'. Accordingly, the transcriptional responses to PbA infection were divided into three categories: genes that are regulated solely by MyD88, by either MyD88 or TRIF or solely by TRIF (Table 1, Supplementary Tables 1 and 2, available at *International Immunology* Online).

Among the genes up-regulated by PbA infection in a MyD88-dependent manner, we noticed that the up-regulation of genes related to TLR-activated microglia cells, such as G-protein-coupled receptor *mFpr-2*, as well as chemokines such as *Ccl3* and *Ccl9*, were also MyD88 dependent, implying that residual microglia or migrated macrophages may also be involved in MyD88-dependent up-regulation of these genes. We found that the genes related to severe malaria, such as *Lipocalin 2* (*24p3*) (35) and *Haptoglobin* (*Hp*), genes associated with cerebral ischemia, such as *C4b* (complement component 4B), *C1qb*, *Klk7* (Kallikrein 7) and *S3-12* (plasma membrane associated protein) and stress response genes, such as *Atf3*, were up-regulated in the brain in a MyD88-dependent manner.

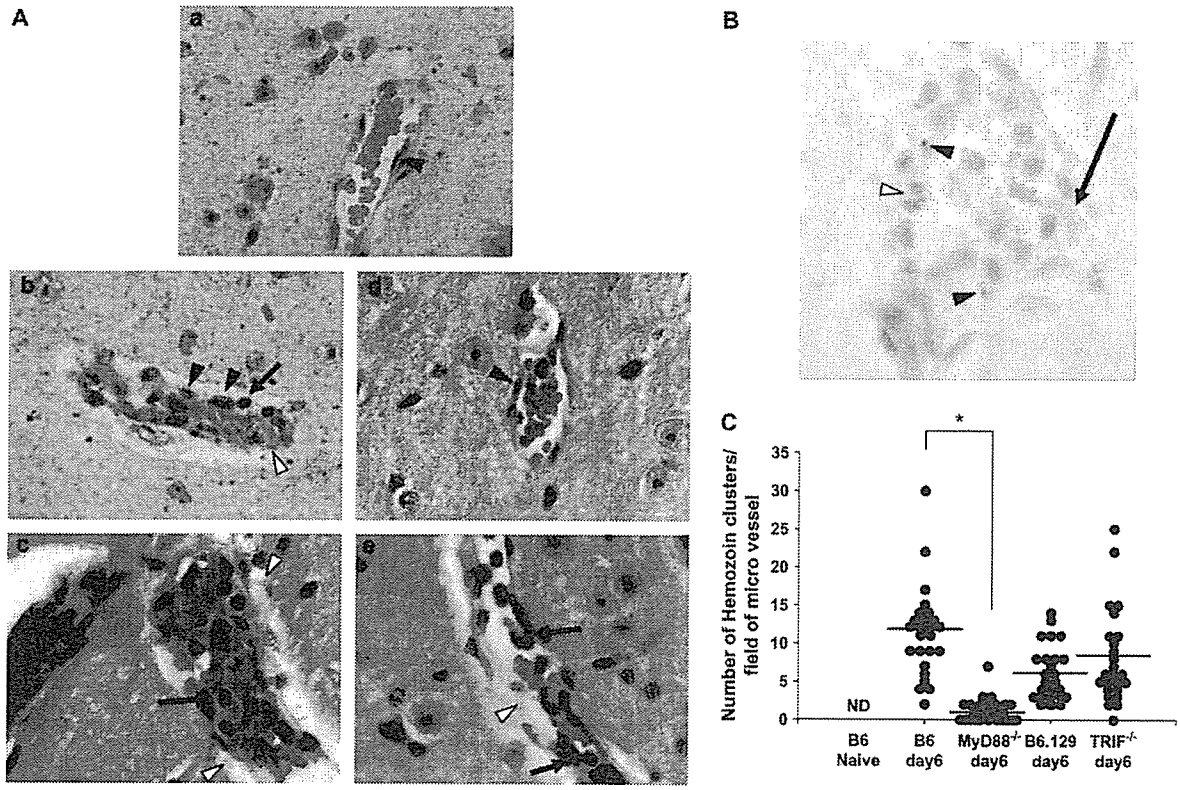

Fig. 2. PbA-infected MyD88-deficient mouse brain displayed a marked decrease in histopathological changes and brain hemozoin load. MyD88$^{-/-}$ and TRIF$^{-/-}$ mice and their WT controls were infected intra-peritoneally with 10^6 RBCs infected with PbA. (A) Histological analysis of brain sections of MyD88$^{-/-}$ and TRIF$^{-/-}$ mice and their WT controls 6 days after PbA infection. Brains were removed and fixed for histological examination. Representative sections from areas around the blood vessels of cerebrum with HE staining are shown ($n = 3$ per group). (a) Normal uninfected mouse brain showing a healthy blood vessel with normal architecture. Endothelial cells (closed triangle, magnification ×1000). (b, c and e) Sections of an infected WT (B6) (b), B6.129 (c) and TRIF$^{-/-}$ (e) mice brains showing severe destruction of endothelial cells (open triangles), sequestration of iRBC (closed triangles) and mononuclear cell infiltration (black arrows, magnification ×1000). (d) Section of an infected MyD88$^{-/-}$ mouse brain showing mostly intact endothelial cells (closed triangle, magnification ×1000) and non-destructed blood vessel. (B) Tissue sections were stained with Prussian blue, and hemozoin clusters were counted by light microscopy. WT brain stained with Prussian blue is shown. Note that shown is a disrupted vessel, with a destruction of endothelial cells (black arrows), and infiltrated mononuclear cells (open triangle) that a counterstaining with nuclear red solution shows very faint staining, but clear visualization of dark brown hemozoin clusters (closed triangle, magnification ×1000). (C) Hemozoin clusters in infiltrated brain vessels were counted in 25 microscopic fields. MyD88$^{-/-}$ mouse brains had significantly lower numbers of hemozoin clusters in each area counted ($P < 0.001$, Mann–Whitney *U*-test, $n = 3$ or 4 per group). ND represents not detected in uninfected naive mice.

We also noted that the genes which are (i) associated with cytotoxicity, such as *Gzmb* (*granzyme B*) and *Pdcd1lg1* (programmed cell death 1 ligand 1, also called B7-H1 or CD274); (ii) related to lymphocyte recruitment, such as *Ccl3*, *Ccl9* and *Ccr5*; (iii) IFN (type-I and/or -II) inducible, such as *Vig1*, *Oasl2*, *Tap-1*, *Ifi44*, *Ifit3*, *Ifi35*, *Isg15*, *Irf7*, *Irf9*, *Usp18*, *Ifi1* (*LRG-47*), *Stat1*, *Mx1*, *Mda5*, *Ppicap* (lectin, also called *CyCAP*) and *Zfp36* and (iv) expressed in T cells and NK cells, such as *Ms4a4b* (also called *Chandra*) (36), *schlafen 1* and *schlafen 2*. These data suggest that type-I or -II IFN-producing immune cells such as T cells, DCs and/or NK cells may be involved in the up-regulation of such genes in the brain during PbA infection.

Some of the up-regulated genes that are dependent on either MyD88 or TRIF include type-II IFN-inducible genes such as *Lmp7*, *Ubiquitin D* (*Ubd*), *H-2Kd*, *Ifi205*, *Gbp2* and *Ifi47* and GTPases and chemokines such as *Ccl5*, *Cxcl10*, *Cxcl9*, *Cxcl16* and *Ccl21a* indicate that there is, in fact, TRIF-dependent, possibly TLR3- and/or TLR4-mediated, innate immune recognition during PbA infection (Supplementary Table 1, available at *International Immunology* Online).

To confirm the results obtained by DNA microarray analysis, some of the gene expression was monitored by RT–PCR in the brain tissues at day 6 after PbA infection. Significant up-regulation of *Granzyme B*, *Lipocalin 2* and *Ccl3* mRNA expression was observed in a MyD88-dependent manner (Fig. 3, $*P < 0.05$ by Student's *t*-test). The results obtained by DNA microarray analysis revealed novel genes that were up-regulated in a MyD88-dependent manner, suggesting their critical role in CM pathogenesis. Importantly, MyD88-dependent